Microchimica Acta (2022) 189: 362
https://doi.org/10.1007/s00604-022-05399-y

REVIEW ARTICLE

A comprehensive review on electrochemical and optical aptasensors for organophosphorus pesticides

Hossein Khosropour[1,2] · Pramod K. Kalambate[1,2] · Rupali P. Kalambate[1,2] · Khageephun Permpoka[1,2] · Xiaohong Zhou[3] · George Y. Chen[4] · Wanida Laiwattanapaisal[1,2]

Received: 21 April 2022 / Accepted: 1 July 2022 / Published online: 31 August 2022

Abstract

There has been a rise in pesticide use as a result of the growing industrialization of agriculture. Organophosphorus pesticides have been widely applied as agricultural and domestic pest control agents for nearly five decades, and they remain as health and environmental hazards in water supplies, vegetables, fruits, and processed foods causing serious foodborne illness. Thus, the rapid and reliable detection of these harmful organophosphorus toxins with excellent sensitivity and selectivity is of utmost importance. Aptasensors are biosensors based on aptamers, which exhibit exceptional recognition capability for a variety of targets. Aptasensors offer numerous advantages over conventional approaches, including increased sensitivity, selectivity, design flexibility, and cost-effectiveness. As a result, interest in developing aptasensors continues to expand. This paper discusses the historical and modern advancements of aptasensors through the use of nanotechnology to enhance the signal, resulting in high sensitivity and detection accuracy. More importantly, this review summarizes the principles and strategies underlying different organophosphorus aptasensors, including electrochemical, electrochemiluminescent, fluorescent, and colorimetric ones.

Keywords Organophosphorus pesticides · Electrochemical aptasensor · Fluorescent aptasensor · Colorimetric aptasensor · Electrochemiluminescent aptasensor

Abbreviations

NH_2-DFNS	Amino-functionalized mesoporous dendritic fibrous nanosilica
AT-TWJ-DNA	AT-rich three-way junction DNA
CE	Capillary electrophoresis
CQDs	Carbon quantum dots
CTAB	Cetyltrimethylammonium bromide
R_{CT}	Charge transfer resistance
CS	Chitosan
CHP	Chlorpyrifos
CM	Colorimetric
cDNA	Complementary DNA
CuNP	Copper nanoparticle
CV	Cyclic voltammetry
DZN	Diazinon
DPV	Differential pulse voltammetry
DMT	Dimethoate

Highlights
- The first review was arranged based on the types of organophosphorus pesticides.
- Detection of organophosphorus pesticides is critical in environmental and agricultural monitoring.
- Electrochemical, fluorescent, and colorimetric aptasensors were investigated.
- Challenges in organophosphorus pesticide detection are presented.

✉ Hossein Khosropour
hossein.k@chula.ac.th

✉ Wanida Laiwattanapaisal
Wanida.L@chula.ac.th

[1] Department of Clinical Chemistry, Faculty of Allied Health Sciences, Chulalongkorn University, Bangkok 10330, Thailand

[2] Biosensors and Bioanalytical Technology for Cells and Innovative Testing Device Research Unit, Chulalongkorn University, Bangkok 10330, Thailand

[3] School of Environment, Tsinghua University, Beijing 100084, China

[4] Shenzhen Key Laboratory of Photonic Devices and Sensing Systems for Internet of Things, Guangdong and Hong Kong Joint Research Centre for Optical Fibre Sensors, Shenzhen University, Shenzhen 518060, China

DMOAP	Dimethyloctadecyl[3-(trimethoxysilyl) propyl]ammonium chloride
DNA-AgNCs	DNA-templated silver nanoclusters
dsDNA	Double-stranded DNA
DLS	Dynamic light scattering
EC	Electrochemical
EIS	Electrochemical impedance spectroscopy
ECL	Electrochemiluminescent
ESR	Electron spin resonance
EDS	Energy dispersive spectroscopy
ELISA	Enzyme-linked immunosorbent assay
Exo I	Exonuclease I
Fc	Ferrocene
FE-SEM	Field emission scanning electron microscopy
FS	Fluorescent
FRET	Fluoresce resonance energy transfer
FTO	Fluorine tin oxide
FT-IR	Fourier transform infrared
GC	Gas chromatography
GC-MS	Gas chromatography-mass spectrometry
GCE	Glassy carbon electrode
Au	Gold
GNP	Gold nanoparticles
GNR	Gold nanorods
GNS	Gold nanostars
g-CN	Graphitic carbon nitride
g-SPE	Graphite screen-printed electrode
G	Graphene
GO	Graphene oxide
GQDs	Graphene quantum dots
HP	Hairpin
h-BN	Hexagonal boron nitride
HPLC-MS	High-pressure liquid chromatography-mass spectrometry
IO	Iron oxide
ICB	Isocarbophos
LOD	Limit of detection
LC-MS	Liquid chromatography-mass spectrometry
LC	Liquid crystal
MLT	Malathion
MS	Mass spectrometry
MC	Mesoporous carbon
MOF	Metal organic framework
MB	Methylene blue
MIP	Molecularly imprinted polymers
MWCNTs	Multiwalled carbon nanotubes
NMM	N-methyl mesoporphyrin IX
OMT	Omethoate
OPs	Organophosphorus pesticides
O-DB	Ortho-dihydroxybenzene
O-PD	Ortho-phenylenediamine
PLNRs	Persistent luminescence nanorods
PEC	Photoelectrochemical
PL	Photoluminescence
PhT	Phorate
PS	Phosphorescence
PE	Platinum electrode
PDDA	Poly(diallyldimethylammonium chloride)
PDA	Polydopamine
PEG	Polyethylene glycol
PGPMA	Poly(N-(3-guanidinopropyl) methacrylamide) homopolymer
PEDOT	Poly-3,4-ethylenedioxythiophene
PFF	Profenofos
QDs	Quantum dots
RGO	Reduced graphene oxide
SEM	Scanning electron microscopy
SPE	Screen-printed electrodes
SPGE	Screen-printed gold electrode
SWCNTs	Single-walled carbon nanotubes
ssDNA	Single-stranded DNA
Ag	Silver
AgNP	Silver nanoparticles
Na_2MoO_4	Sodium molybdate
SWV	Square wave voltammetry
SPR	Surface plasmon resonance
Tb-MOF	Terbium(III)-metal organic framework
Tn	Thionine
TEM	Transmission electron microscopy
T7 Exo	T7 exonuclease
UCNPs	Upconversion nanoparticles
USEPA	US Environmental Protection Agency
VS_2QDs	Vanadium disulfide quantum dots
WS	Walking strand
WHO	World Health Organization
GOPS	(3-Glycidyloxypropyl)trimethoxysilane
TMB	3,3′,5,5′-Tetramethylbenzidine

Introduction

Nowadays, different types of agricultural pesticides are widely applied to increase crop yield and product quality [1–3]. Pesticides are used to control the spread of infesting species in order to boost agricultural yield. The use of pesticides is expected to add approximately 30% to crop production worldwide [4]. While their use might boost agricultural yields, their presence in water, fruits, vegetables, and meals can have a detrimental effect on human health globally, causing diseases such as cancer, acute intoxication, neurological ailments, asthma, and allergies [5–7]. These organic and synthetic compounds are usually classified based on their chemical structure into four main groups: organophosphorus, organochlorines, pyrethroids, and carbamates pesticides [8]. Among these four groups, OPs account for more than

30% of all pesticides on the market [9]. These substances are frequently used in pest management and consequently infiltrate the food industry in a variety of ways, posing health risks to people [10]. Pesticides are mostly absorbed through the skin, ingestion, and inhalation. Agriculturists, pesticide sprayers, and loaders, as well as residents living near agricultural land where pesticides are often sprayed on crops, are impacted by pesticides by direct skin penetration or inhalation. On the other hand, humans are indirectly impacted when they consume pesticide-contaminated food. Therefore, detecting and monitoring these compounds is a major challenge for the advancement of human health. The residual OP detection in the food industry, humans, and animals is critical to manage and control their contamination. So far, OP residues have been detected using various methods, such as LC–MS [11–13], GC–MS [14–16], CE [17–19], and ELISA [20, 21]. Despite their high sensitivity and accuracy, these approaches involve extensive sample preparation, time-consuming analysis, and expensive precision tools and trained staff. Biosensors are very attractive due to their ability to detect environmental pollutants, pathogens, and a variety of chemical/biological compounds accurately and rapidly.

Antibody and aptamer are the two recognition components that meet the needs of high sensitivity, remarkable selectivity, and rapid reaction. Antigen–antibody-specific binding has been widely used in biosensors. However, antibodies against smaller molecules and molecules with a high toxicity are difficult to acquire, limiting its application. Alternatively, aptamers exhibit an excellent affinity and selectivity for small molecules and are more stable than antibodies. Aptasensors use a single-stranded oligonucleotide (aptamer) that reacts specifically with the species [22–25]. Bonding can occur through various reactions, including π-π stacking, electrostatic, and hydrogen bonds [26–28]. Owing to their target specific binding various aptamer-based biosensors have been designed for qualitative and quantitative monitoring. The addition of nanomaterials to the surface of aptamer-based biosensors has facilitated the use of biosensors. The target-specific characteristics of aptasensors enable the cost-effective, efficient, rapid, and accurate monitoring of different food contaminants. Hence, aptamers have been widely utilized in biosensors [29–36]. Aptasensors come in a variety of configurations; we focused on EC and optical aptasensors.

The continuous concerns over OPs have become more alarming all over the world due to their detrimental effects on human health. Due to these concerns, several types of aptasensors were developed based on various detection techniques, such as EC and optical. EC and optical sensors continue to limit the capacity to detect several OP residues using a single sensor. Hence, to overcome these challenges, more research should be focused on the use of aptasensors for OP detection, which is still in its infancy due to the restricted number of aptamers that have been developed so far. As a result, much work is required to fabricate environmentally safe, long-lasting, cost-effective, and robust sensing devices for real-time OP residue analysis. We believe there is still opportunity for new research and review articles in this field for the stated reasons. This review summarizes the construction of aptamers used in recent years to detect OPs with challenges and prospects for building high-performance novel OP residue aptasensors. The development of an aptamer-based experiment to detect OPs in real samples could facilitate experiments on agricultural products. Table 1 describes the aptamers used to detect OPs.

Types of aptasensors for organophosphorus pesticides

Aptasensors are thermally stable and can be synthesized in vivo. Their structural modifications are possible by rehybridization and denaturalization with various functional groups. In recent years, various aptasensors such as EC, ECL, FS, and CM have been employed to detect OP residues. EC and FS aptasensors have been major candidates for OP detection because of their rapid response, high sensitivity, outstanding properties, and low cost.

Electrochemical aptasensors

EC aptasensors generate a signal in response to the binding of a specific target substance, which is recorded

Table 1 Specific aptamers for OP determination

OPs	Sequence	K_D	Ref
CHP	CCTGCCACGCTCCGCAAGCTTAGGGTTACGCCTGCAGCGATTCTTGATCGCGCTGCTGGTAATCCTTCT TTAAGCTTGGCACCCGCATCT	-	[33]
MLT	ATCCGTCACACCTGCTCTTATACACAATTGTTTTTCTCTTAACTTCTTGACTGCTGGTGTTGGCTCCCG TAT	-	[34]
DZN	ATCCGTCACACCTGCTCTAATATAGAGGTATTGCTCTTGGACAAGGTACAGGGATGGTGTTGGCTCCCG TAT	55.5 μmol L^{-1}	[35]
ICB	AAGCTTGCTTTATAGCCTGCAGCGATTCTTGATCGGAAAAGGCTGAGAGCTACGC	0.8 μmol L^{-1}	[36]
PhT	AAGCTTGCTTTATAGCCTGCAGCGATTCTTGATCGGAAAAGGCTGAGAGCTACGC	1.1 μmol L^{-1}	[36]
PFF	AAGCTTGCTTTATAGCCTGCAGCGATTCTTGATCGGAAAAGGCTGAGAGCTACGC	1.0 μmol L^{-1}	[36]
OMT	AAGCTTTTTTGACTGACTGCAGCGATTCTTGATCGCCACGGTCTGGAAAAAGAG	2.0 μmol L^{-1}	[36]

electrochemically. Three important steps are followed in designing an EC aptasensor: the use of nanomaterials for signal amplification, aptamer binding, and sensing. In these aptasensors, the most common method of binding an aptamer to the surface is covalent bond formation [37].

Fluorescence aptasensors

FS aptasensors are one of the most often utilized sensing candidates due to their great sensitivity and simplicity. Fluorescence is a photon emission process that occurs when a fluorophore is stimulated with an excitation light and is influenced by the surrounding environment. Then, signal changes are collected and observed by a spectrophotometer. FS aptasensors have two main types of signal measurement: "on" and "off" signals. By leveraging the benefits of nanoparticles and tailoring the FS intensity to the target binding, they are able to detect OPs [38].

Colorimetric aptasensors

The primary advantage of CM sensing is its simplicity and ease of use. CM aptasensors have been widely used to detect OPs contaminants in real samples because of they allow observation by the naked eye. Therefore, the primary difficulty in constructing CM sensors is transforming response change to visual color change. Au and Ag nanoparticles are the most frequently used probes in CM assays. These nanoparticles, due to their capacity to amplify the plasmon surface, help to produce appropriate signals in colorimetry [39, 40].

Electrochemiluminescent aptasensors

Electrochemiluminescence produces photons in the UV, visible, and near IR. Here, the light is emitted from the EC reaction as the electrogenerated luminescence which is directly proportional to the concentration of the reactant. The ECL luminophore generated at the electrode surface undergoes high-energy electron transfer processes, resulting in the generation of electrically excited states, or luminescent signals. Luminophores such as luminol and QDs are commonly employed. The advantages of ECL over other techniques are low background noise, low background emission, rapidity, and high sensitivity.

Detection of organophosphorus pesticides

Chlorpyrifos

CHP was first produced by Dow Chemical in the USA in 1966 and marketed under various brands such as Lorsban and Dursban [41, 42]. It has been used as OPs with a wide range of uses to kill pests such as lice, flies, and herb pests in agricultural and residential environments [43]. Improper use of CHP causes high toxicity and adverse effects on aquatic organisms and humans [44]. Appropriate amounts of CHP have been measured in real samples by using chromatographic techniques, such as GC–MS and LC–MS [45–48]. Despite their excellent accuracy, current methods for measuring CHP are expensive and time consuming.

Two simplest EC aptasensors were designed by Jiao and coworkers. In the first study, Jiao et al. [49] designed an EC aptasensor for CHP detection via CV analysis of calibration curve with MC functionalized by CS, Fc, and MWCNTs (Fc@MWCNTs-CS) (Fig. 1A). Fc@MWCNTs-CS was constructed with a simple dispersion strategy and the CV responses of several electrodes were investigated in potassium hexacyanoferrate(III/II). In this study, CS-functionalized MC has a high specific surface area, high porosity, and excellent dispersibility, all of which were employed to efficiently capture larger volumes of material. The linear range and LOD for CHP detection using CV were $1–1\times10^5$ ng mL^{-1} and 0.33 ng mL^{-1} (S/N = 3), respectively. In another study, Jiao et al. [50] developed a CV aptasensor with GO@Fe_3O_4 on a GCE to detect CHP in vegetable samples. GO@Fe_3O_4 was constructed with a simple solvothermal process. In this case, the nanocomposite of GO and Fe_3O_4 formed a unique sensing film that had strong synergistic effect. The GO provided high surface area [51], and Fe_3O_4 nanoparticles were evenly deposited on the GO surface, which made it possible to detect CHP with high sensitivity and low LOD. The LOD and linear range of CHP detection was 0.033 ng mL^{-1} and $0.1–1.0\times10^5$ ng mL^{-1}, respectively.

Xu et al. [52] designed a sensitive and selective EC aptasensor via an NH_2-captured aptamer probe and a CHP aptamer with copper oxide nanoflowers-SWCNTs on GCE in spiked celery, cabbage, and apple samples (Fig. 1B). Because of their high electrocatalytic activity, copper oxide nanoparticles have received a lot of attention for signal amplification [53–55]. MB, a redox indicator for DNA hybridization, can bind with nucleic acid chains in a non-covalent manner [56]. This was shown with the DPV method. The obtained results showed a linear range of 0.1–150 ng mL^{-1} and a LOD of 70 pg mL^{-1}, respectively. Based on our opinion, this superior sensing capability can be due to the high surface-to-volume ratio of three-dimensional CuO NFs and the synergistic effect of CuO NFs and SWCNT electrical conductivity.

A sensitive voltammetric MIP aptasensor with GNR as an enhancing agent on a GCE was constructed by Roushani et al. [57]. O–PD and O-DB were used as monomers to prepare a MIP on the surface of a GCE modified with GNR (Fig. 1C). After electropolymerization, the films formed on the surface had suitable groups such as –OH and –NH, which caused the formation of effective sites for reaction [58]. The LOD and linear range

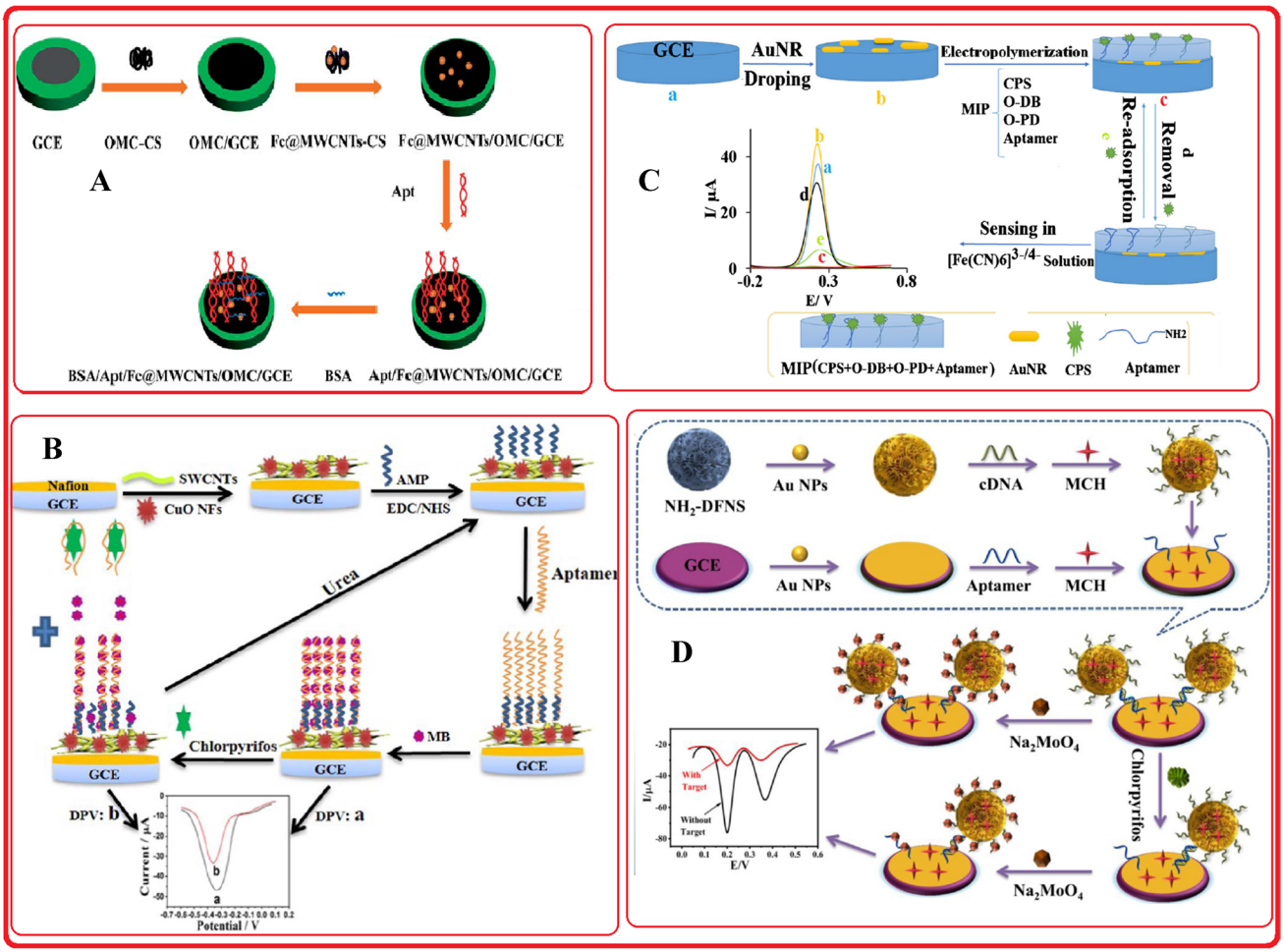

Fig. 1 **A** Schematic preparation of the EC aptasensor for CHP detection by Jiao et al. [49]. **B** Schematic step-by-step preparation of the EC aptasensor for CHP detection by Xu et al. [52], **C** schematic preparation of the EC aptasensor for CHP detection by Roushani et al. [57], and **D** schematic step-by-step preparation of the EC aptasensor by Na_2MoO_4 with phosphate of ssDNA as a used signal generation for CHP detection by Liu et al. [59]. Reprinted with permission from [49, 52, 57], and [59]

of this MIP aptasensor were 0.35 fmol L^{-1} and 1.0 fmol L^{-1}–0.4 pmol L^{-1}, respectively. This MIP aptasensor displayed good recovery (97.6–103.2%) in lettuce and apple samples.

Liu et al. [59] reported a CHP aptasensor that utilizes aptamer as both a capture and signaling molecule. Here, the phosphate from the aptamer reacts with molybdate to form molybdophosphate precipitate, which generates an EC signal. The aptasensor is composed of NH_2-DFNS and GNP. In this study, the mesoporous dendritic fibrous nanosilica is sphere-shaped with three-dimensional central radial channels and hierarchical pores. It has a higher specific surface area and larger pore volume, which increases signal intensity and sensitivity of detection. Figure 1D shows the SWV response of Na_2MoO_4 with phosphate in ssDNA as a used signal generation. The proposed SWV aptasensor displayed a linear range and LOD from 1.0 fmol L^{-1} to 1.0 nmol L^{-1} and 0.43 fmol L^{-1}, respectively.

Lin et al. [60] have recently constructed a turn-on DPV aptasensor for CHP detection by electrodepositing GNP on 2D-Mo_2C/Mo_2N composites. The Fc aptamer probe and CHP aptamer make a dsDNA structure and connect with Au on the electrode surface via Au–S bonds. The CHP aptamer separates from the Fc probe aptamer in the presence of CHP. Therefore, this action increases the Fc current peak in the EC aptasensor. The method displayed a linear dynamic range and LOD of 0.1 to 400 ng mL^{-1} and 0.036 ng mL^{-1} CHP, respectively. The selectivity of the aptasensor was acceptable in the presence of atrazine, amitrole, fenitrothion, and carbendazim as interference pesticides. The determination of CHP in pak choi and apple samples displayed good recovery and RSD ranges of 94.7–116.7% and 2.57–7.08%, respectively.

A signal-on FS aptasensor for CHP, MLT, and DZN detection was designed by Cheng et al. [61]. QD nanobeads and GNS as a fluorophore quencher were developed to

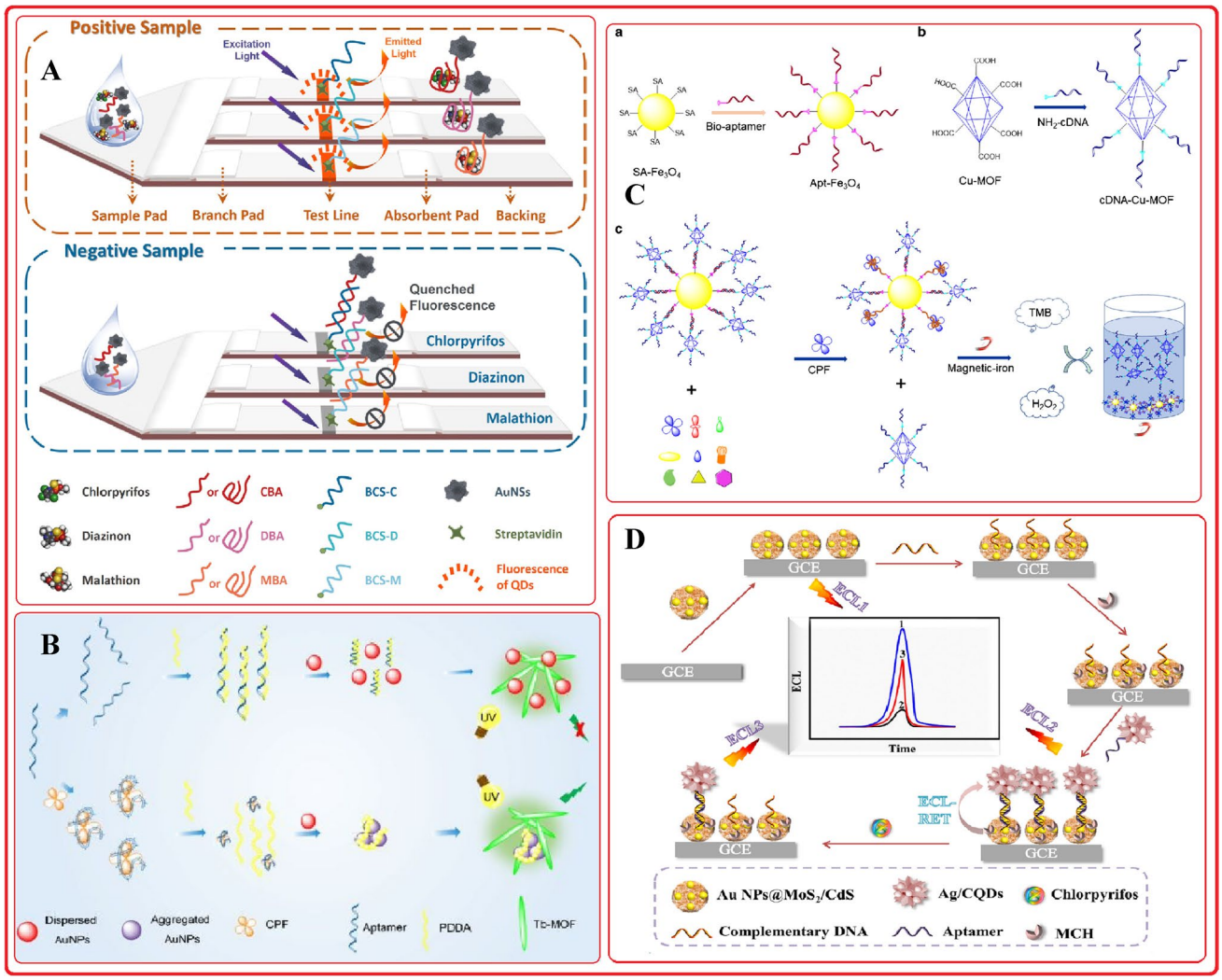

Fig. 2 **A** FS aptasensor for multi-pesticide detection by Cheng et al. [61], **B** FS process of CHP detection based on Tb-MOF@PDDA aggregated-GNP by Liu et al. [62], **C** schematic process of CM aptasensor for CHP detection by Liu et al. [63], and **D** schematic process of ECL aptasensor for CHP detection by Liu et al. [64]. Reprinted with permission from [61–63], and [64]

detect the above pesticides in real samples, such as spinach and cabbage (Fig. 2A). The LOD values of 0.73, 6.7, and 0.74 ng mL^{-1} were obtained for of CHP, DZN, and MLT, respectively. The capability for multi-pesticide detection of the aptasensor was examined by recovery studies (82.4–112.8%). This sensitive FS aptasensor has the potential to become a valuable tool for on-site multi-pesticide quantification.

In another FS investigation, Liu et al. [62] studied CHP detection with Tb-MOF and PDDA-aggregated-GNP. In this study, Tb-based MOF possess exceptional luminous characteristics and are therefore employed as a FS probe. Figure 2B shows the step-by-step quenching FS process between GNP and Tb-MOF. The CHP-aptamer complex forms after the addition of CHP, and then, PDDA causes GNP to aggregate. The proposed aptasensor detected CHP sensitively with LOD and linear range of 3.8 and 5–600 nmol L^{-1}, respectively. Finally, this aptasensing platform could successfully determine CHP in some fruit and vegetable samples with acceptable recovery (82.2–93.6%).

Liu et al. [63] developed a Cu-MOF-based CM aptasensor for the sensitive detection of CHP by affixing CM labels to the magnetic carrier through the hybridization reaction between the cDNA probe and the CHP aptamer. The authors developed the color using a Cu-MOF reactor catalytic TMB-H_2O_2 system. The color of TMB/H_2O_2 changes with CHP incubation on the aptamer via UV–Vis spectrophotometry (650 nm) (Fig. 2C). The Cu-MOF-based aptasensor displayed appropriate LOD (4.4 ng mL^{-1}) and linear range (0–1250 ng mL^{-1}) for CHP detection. In addition, the current CM aptasensor has been selectively applied to detect CM in vegetable

and fruit samples with lower than 5% RSD and higher than 91% recovery.

In the last paper for CHP detection, Liu et al. [64] designed a signal-on ECL aptasensor with MoS_2/CdS nanospheres and Ag/CQDs. Ag/CQDs and MoS_2/CdS nanospheres as receptor and light emitter, respectively, were used for effective ECL resonance energy transfer (Fig. 2D). The ECL potential was occurred on modified electrode in pH 7.4 at 0.1 M PBS and $K_2S_2O_8$. In this study, the high luminescence intensity can occur on $K_2S_2O_8$ with a large specific surface area and electron density of MoS_2/CdS nanospheres. Under optimal conditions, the range of CHP determination was 10 nmol L^{-1}–1.0 fmol L^{-1}, and the LOD was 0.35 fmol L^{-1}. The performance of the ECL aptasensor was evaluated using HPLC–MS with lower than 5% RSD and higher than 96% recovery in vegetable and fruit samples.

Malathion

MLT is another OP [65] that, if used in large amounts, can cause neurological [66, 67], metabolic [68, 69], reproductive, and growth [70, 71] disorders. It is also commonly used to control and kill insects such as *Ceratitis capitata* that attacks fruits, vegetables, and grains. Numerous studies worldwide showed that many rivers, such as Central Amazon River [72, 73], the Nile River in Egypt [74], the Babool River in Iran [75], and the Mediterranean coast [76], are contaminated with MLT. This insecticide is one of the most widely used insecticides on the planet. Numerous methods, such as CE [77], GC [78, 79], HPLC [80, 81], GC–MS [82], and HPLC–MS [83, 84], have been applied for MLT detection.

Prabhakar et al. [85] designed a simple DPV aptasensor for MLT detection by depositing CS and IO nanoparticles on FTO. In this study, IO nanoparticles got a lot of attention because they can improve conductivity, superparamagnetism, and signal amplification, which imply they can improve sensitivity and selectivity [86, 87]. IO nanoparticles were synthesized using $FeCl_2$ and $FeCl_3$ with co-precipitation method [88]. The biotinylated MLT aptamer as a ssDNA structure was connected with streptavidin on modified electrode surface via streptavidin-S interaction. For MLT detection, this aptasensor had a linear dynamic range of 0.001 ng mL^{-1} to 0.01 µg mL^{-1}. The determination of MLT in soil and lettuce leave samples displayed good recoveries approximately 80–92%.

In another investigation, Xu et al. [89] focused on the dual-signal determination of MLT with an EC aptasensor. They modified GCE with PDA-GNP and Exo I. In addition, Au connected with a 3´-SH capture aptamer probe (Fig. 3A). The HP probe was modified to include labels for Fc and Tn with an amino group as a second signal at the aptamer. We believe that using two electrochemical responses (Fc and Tn) simultaneously to detect changes in MLT concentration is a suitable strategy for MLT determination with high accuracy and precision. SEM results of PDA displayed polymerized DA uniformly on the GCE and made an acceptable platform for the functional modification of material surface [90, 91]. The results displayed two signal responses: signal-on and off for Fc and Tn, respectively. The proposed aptasensor had LOD, linear range, stability, and reproducibility for MLT of 0.5 ng L^{-1}, 0.5–600 ng L^{-1}, 4.48%, and 6.72%, respectively. Good and acceptable results of recovery (96.10–108.29%) and RSD (1.04–6.14%) were obtained in cauliflower and cabbage analyses.

Kaur et al. [92] developed a DPV aptasensor for MLT detection using PEDOT and carboxylated MWCNTs on FTO sheets by chronoamperometry at a potential of 1.0 V for 3 min (Fig. 3B). In this study, the PEDOT-MWCNTs hybrid film has a high electrical conductivity, improved mechanical stability, and fast electron transfer kinetics [93]. Therefore, the use of this hybrid has been able to create a suitable aptasensor for MLT determination. The proposed DPV aptasensor for MLT detection displayed LOD, linear range, and sensitivity of 0.5 fmol L^{-1}, 0.1 fmol L^{-1}–1.0 µmol L^{-1}, and 27 µA/(fmol L^{-1}) cm^{-2}, respectively. Finally, the aptasensor was validated by comparison with HPLC in spiked lettuce sample with 95–100% recovery and 0.43–3.81% RSD.

In another study, a zirconium-MOF nanocomposite was synthesized as a probe for an EC aptasensor for MLT detection by Xu et al. [95]. Zirconium-MOF has attracted attention in EC applications because of its outstanding catalytic characteristics, thermal stability, and good electrical properties. It was connected with 5′-NH_2-cDNA and carboxylated Fc. The 5′-SH-MLT aptamer was connected with Au–S bond on GNP-GCE, and it formed a dsDNA structure with the cDNA of the nanocomposite probe. Finally, the nanocomposite probe was removed in the Tris–HCl buffer after adding MLT because of the strong connection of the MLT aptamer with the pesticide. This EC aptasensor exhibited a linear range and LOD of 25–850 and 17.18 ng L^{-1}, respectively. The proposed aptasensor had an acceptable recovery and RSD for MLT detection in long bean and cucumber samples.

Bala et al. [96] reported a sensitive FS aptasensor for MLT determination, with a LOD and linear range of 4 pmol L^{-1} and 0.01 nmol L^{-1}–1 µmol L^{-1}, respectively, via the FS response of CdTe@CdS-QDs and PGPMA as a probe. The signal of FS switched off after adding MLT to PBS buffer pH = 7.32 because of the presence of cationic polymer and quenched QDs. However, before the addition of MLT, the aptamer and the polymer were connected by electrostatic interactions, and the polymer did not affect the FS of QDs

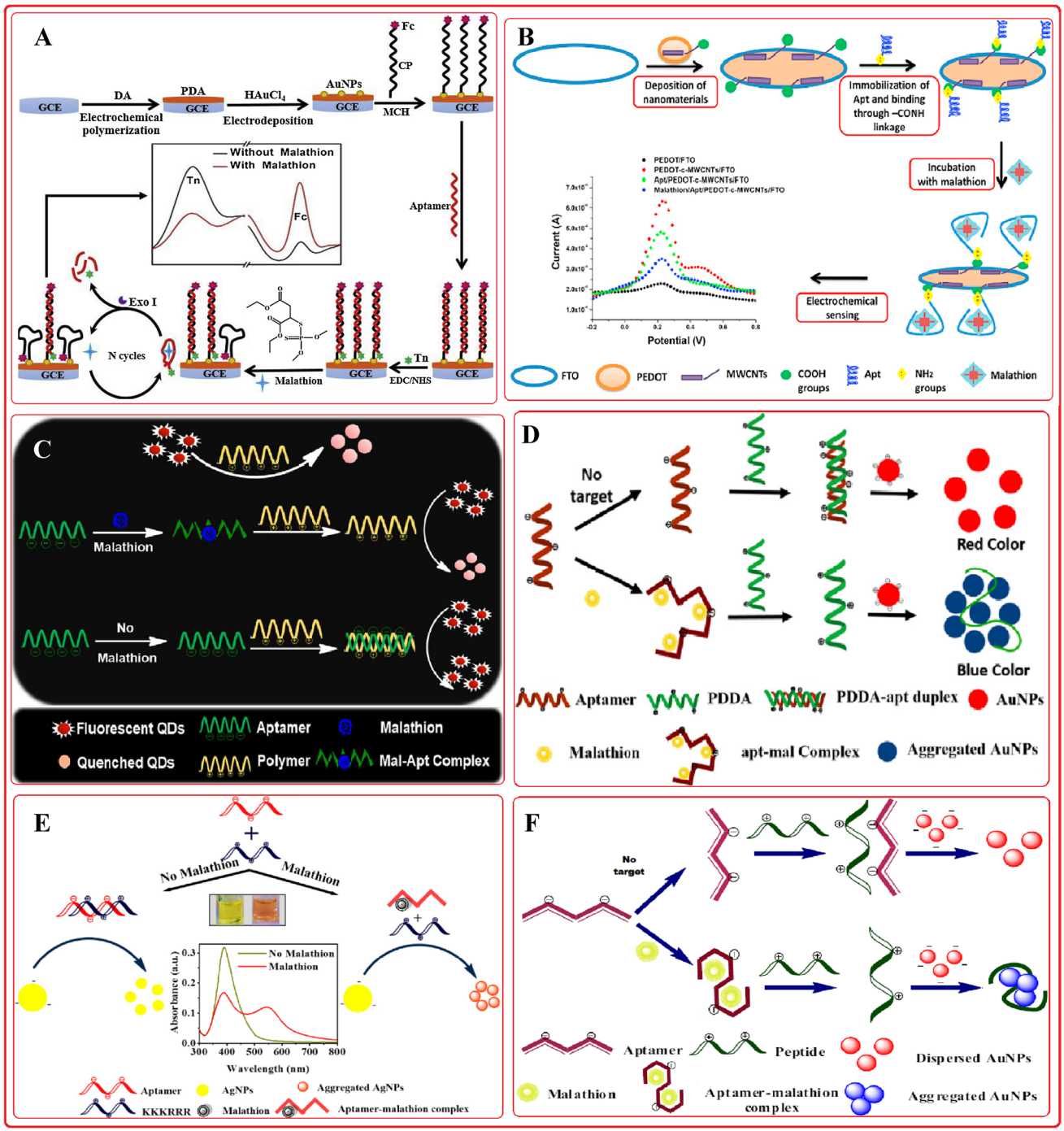

Fig. 3 **A** EC process of MLT detection based on PDA-GNP by Xu et al. [89], **B** schematic process of DPV aptasensor for MLT detection by Kaur et al. [92], **C** FS process of MLT detection based on CdTe@CdS-QDs and PGPMA by Bala et al. [96], **D** CM process of MLT detection based on unmodified GNPs and PDDA by Bala et al. [40], **E** schematic process of CM aptasensor for MLT detection by Bala et al. [9], and **F** schematic process of CM aptasensor reported by Bala et al. (2018) [98]. Reprinted with permission from [9, 40, 89, 92, 96], and [98]

(Fig. 3C). Finally, the proposed FS aptasensor was successfully applied for MLT detection in three types of water and orange samples with acceptable recovery (84–119%).

In the last investigation, Chen et al. [97] reported a sensitive turn-off FS aptasensor combining $NaYF_4$:Yb, Er UCNPs, GNPs, and PDDA as a negative, positive, and positive charge structure, respectively, to prepare FRET after the

addition of MLT. The FS response decreased with increasing MLT concentration in the linear range of 0.01–1 µmol L^{-1}. Moreover, the obtained LOD was 1.42 nmol L^{-1}. Finally, the developed aptasensor displayed acceptable results for MLT determination such as recovery (90.00–111.75%) in tap water and tea powder samples.

Bala et al. [40] applied unmodified GNPs and PDDA as a water-soluble and cationic polymer for a sensitive CM aptasensing platform for determination of MLT. Here, the role of PDDA is important before and after the addition of MLT. Prior to the inclusion of MLT, the MLT aptamer interacts with PDDA, resulting in the red dispersion of free GNP. After addition of MLT, PDDA interacted with the free GNP and the color changed from red to blue (Fig. 3D). The developed CM aptasensor had a linear range and LOD of 0.5–1000 and 0.06 pmol L^{-1}, respectively. At last, this aptasensing platform was examined by comparison with HPLC for MLT determination in apple and lake water samples with (88–104%) recovery and (3.08–7.91%) RSD.

In another study, Bala et al. [9] used unmodified GNP with a positively charged peptide as a linker to the MLT-aptamer (before addition MLT) and to the GNP (after addition MLT) for a sensitive CM aptasensor of MLT detection (Fig. 3E). For MLT detection, the unmodified GNP/peptide-based CM aptasensor showed a good linear range (0.01–0.75 nmol L^{-1}) and LOD (1.94 pmol L^{-1}). This aptasensor was used in two types of water and apple samples with acceptable results.

A sensitive CM aptasensor was reported by Bala et al. [98] using hexapeptide and AgNP for MLT detection. Hexapeptide was chosen for this investigation because it interacts more efficiently with aptamer than other small peptides. Contrary to this, as AgNP has a greater molar extinction coefficient, it offers improved sensitivity and visibility. Here, the hexapeptide interacted with the MLT-aptamer and AgNP before and after the addition of MLT (Fig. 3F). With increasing MLT concentration from 0.01 nmol L^{-1} to 0.75 nmol L^{-1} linearly, the color of the solution changed from yellow to orange. Also, the LOD was found to be 0.5 pmol L^{-1}. Finally, the aptasensor was examined for MLT detection in spiked apple, tap water, and lake water samples with (89–120%) recovery and (2.98–4.78%) RSD.

In the last investigation of MLT detection, Abnous et al. [99] reported a CM aptasensor via protecting GNP with a dsDNA (MLT-aptamer and cDNA). The MLT-aptamer releases cDNA with increasing MLT concentration and then separates from the GNP surface. At last, the GNP aggregate in the presence of salt by changing color from red to purple. In this study, the presence of dsDNA protects the GNP from salt-induced aggregation and improves assay sensitivity by stabilizing the GNP. The LOD and linear response of MLT were 1 pmol L^{-1} and 5 pmol L^{-1}–10 nmol L^{-1}, respectively. With 88.6–104.5% recovery and 1.9–6.8% RSD, this aptasensing technology was effectively employed to determine MLT in serum samples.

The ECL aptasensor developed by Chen et al. [100] was also used for MLT detection. They applied NH_2-MIL-88(Fe) MOF and CdTe QDs-$S_2O_8^{2-}$ for determination of MLT. The QDs are located on the outer and inner structures of the desired MOF. The MLT-aptamer was adsorbed on NH_2-MIL-88(Fe)/CdTe QDs to prepare a nanocomposite ECL probe. When the Fe(II) in NH_2-MIL-88(Fe) reacted with peroxydisulfate ion ($S_2O_8^{2-}$), generated Fe(III) from this reaction was reduced in the EC process. Moreover, the sulfate radical produced in this cycle reacted with CdTe QDs and created a better ECL signal. The results showed a linear range with the logarithm of the MLT concentration in the range of 1 pg L^{-1}–1 µg L^{-1}, with a LOD of 0.3 pg L^{-1}.

In another investigation, Liu et al. [101] designed an ECL simultaneous aptasensor for determination of acetamiprid and MLT determination via g-C_3N_4 and luminol on hollow Cu/Co-MOF as luminescence signals. The hollow MOF was used as the luminescent reagent carrier, which increased the amount of luminescent reagent that could be loaded into the hollow MOF. Its high conductivity improved the luminescent efficiency of reagent, hence enhancing the sensitivity of the assay. They designed a dual-signal ECL aptasensor with luminol and g-C_3N_4 at 0.6 V (acetamiprid) and − 1.5 V (MLT), respectively. The LODs and linear ranges of the dual-signal aptasensor for acetamiprid and MLT detection were 0.015 pmol L^{-1}, 0.018 pmol L^{-1}, and 0.1 pmol L^{-1}–0.1 µmol L^{-1}, respectively. The suggested approach yielded good results for acetamiprid and MLT detection in apple and tomato samples, with recovery of 94–102% and RSD of 2.25–4.28%.

Chen et al. [102] designed a DNA-Ag nanocluster probe for MLT detection by a UV–Vis absorbance aptasensor. The DNA-Ag probe had a maximum absorption at 420 nm, which increased to 420 nm after adding MLT. The proposed aptasensor was used for the sensitive determination of MLT from 0 to 25 µg mL^{-1} by UV–Vis absorbance spectroscopy with a LOD of 25 pg mL^{-1}. Finally, the aptasensor was examined by comparison with HPLC for MLT detection in blood samples.

Another type of optical sensors is LC sensors which Kim Hong and Jang [103] and Nguyen and Jang [104] reported for the sensitive detection of MLT.

Diazinon

Another widely used OPs is DZN (dimethylene isopropyl methyl primidyl thiosulfate), which is used in agriculture to control pests of crops such as fruits and vegetables [105]. It is highly soluble in water, and hence, it has the potential to penetrate the soil and contaminate ground water [106]. This pesticide is classified as a relatively dangerous toxin by the

WHO and the USEPA [107, 108]. DZN is absorbed through the skin of living organisms. More than 350 mg kg^{-1} is lethal to humans [108]. Contamination of the body with DZN changes the amount of liver enzymes, which leads to short-term and long-term effects on humans [109]. Short-term side effects of DZN infection include dizziness, headache, diplopia, nausea, abdominal pain, and skin problems, and long-term side effects include neurological disorders, infertility, and cancer [110, 111]. Therefore, accurate measurement of DZN in water, soil, and crops is crucial to prevent health hazards. In recent years, many methods such as GC and LC [112–118] as well as CE [119] have been used to measure DZN.

Hassani et al. [120] investigated the development of DPV aptasensor for the determination of DZN. This aptasensor was built with a SPGE that had been modified with thiolated aptamers adsorbed on GNP (Fig. 4A). The best deposition time was 150 s. DPV was used to measure EC activity in a $[Fe(CN)_6]^{3-/4-}$ solution. The current fluctuation was investigated in the DZN concentration range of 0.1–1000 nmol L^{-1}. When compared with HPLC and other CM techniques for DZN detection, the proposed aptasensor exhibited an exceedingly low LOD (0.0169 nmol L^{-1}).

Khosropour et al. [121] developed an EC aptasensor to determine DZN. As a novel category of nanocomposite, VS_2QDs were produced using a simple hydrothermal technique and doped on G nanoplatelets/carboxylated-MWCNTs. Through electrostatic contact, the produced nanocomposite on GCE was incubated with the DZN-aptamer. The modified electrode was utilized to detect DZN at low levels by monitoring the oxidation of the redox probe $[Fe(CN)_6]^{3-/4-}$ (Fig. 4B). The DZN-aptamer can preferentially adsorb DZN on the modified electrode, decreasing the DPV current and increasing the R_{CT} of EIS. Under optimum conditions, the developed EC aptasensor has low LOD values of 11 and 2 fmol L^{-1}, respectively, with broad linear dynamic ranges of 50 fmol L^{-1}–10 nmol L^{-1} and 10 fmol L^{-1}–10 nmol L^{-1} for DPV and EIS calibration curves.

Arvand and Mirroshandel [122] created a new aptasensor that detects DZN with high sensitivity and specificity using FRET between QDs as a donor and GO as an acceptor. FRET was used to obtain PL quenching after GO was linked

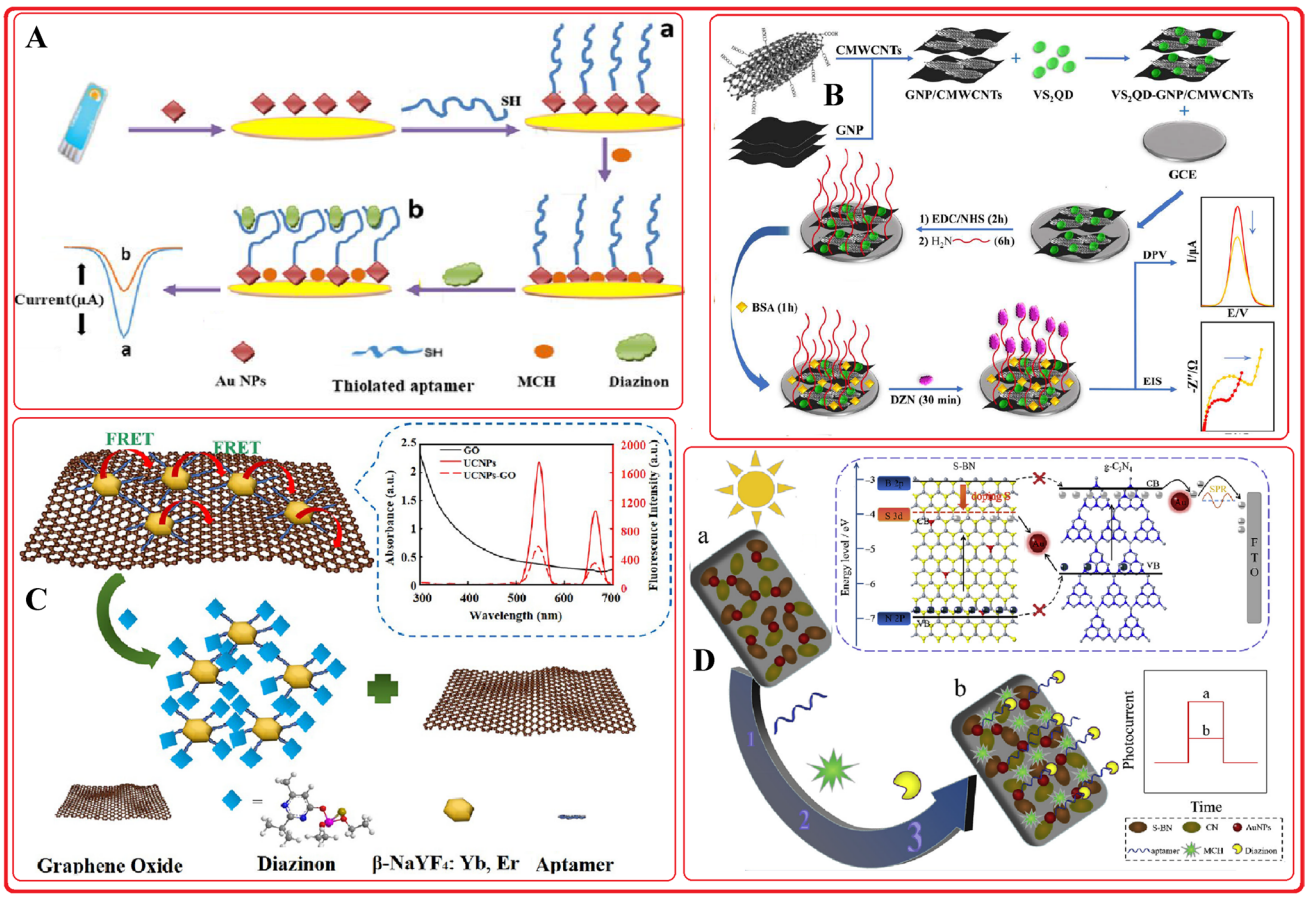

Fig. 4 **A** EC process of DZN detection based on GNP-SPGE by Hassani et al. [120], **B** schematic process of DPV and EIS aptasensor for DZN detection by Khosropour et al. [121], **C** FS process of DZN detection based on GO-UCNP by Rong et al. [123], and **D** PEC process of DZN detection by Tan et al. [125]. Reprinted with permission from [120, 121, 123], and [125]

to aptamers. The LOD of the aptasensors was 0.13 nmol L^{-1}, and its linearity was maintained at 1.05–206 nmol L^{-1}. Due to a lack of binding affinity for the aptamers, other pesticides did not contribute to PL recovery, demonstrating the selectivity of biosensor.

Rong et al. [123] devised a FS aptasensor for detecting DZN in food at low concentrations. Aptamer-modified UCNPs were produced and conjugated with GO through π-π interaction. The FS was quenched because of the FRET between UCNPs and GO. When DZN was added, the aptamer preferred to bind to it, which resulted in the separation of GO and increase in FS signal (Fig. 4C). In this study, the presence of GO due to the high surface area and the placement of a large volume of UCNPs on its surface increase the sensitivity in DZN detection. A wide linear detection range of 0.05–500 ng mL^{-1} and a LOD of 0.023 ng mL^{-1} were achieved under ideal conditions.

Fooladi Talari et al. [124] constructed a FS aptasensor based on reduced GQDs and MWCNTs for DZN detection. A simple FS method using reduced GQDs, a DZN-aptamer, and MWCNTs was developed to measure DZN with a LOD of 0.4 nmol L^{-1} in the range of 4–31 nmol L^{-1}. The proposed aptasensor was able to detect DZN with excellent accuracy and selectivity in real samples. The precise aptasensor created in this study serves as a sensitive, low-cost, quick, and portable device for detecting DZN in contaminated samples.

Tan et al. [125] created a self-PEC aptasensor based on h-BN for DZN detection with high photoelectric conversion efficiency. In this study, the h-BN is a 2D semiconductor comparable to G, but with carbon atoms replaced with boron and nitrogen atoms. However, h-BN can only be excited by ultraviolet light because it has a large bandgap. This hugely limits the use of visible light, so element doping has been an important way to improve the absorption of visible light and to narrow the bandgap of photoactive materials. With an original concept to establish a Z-scheme heterojunction of h-BN and gCN by doping sulfur into h-BN, they were the first to use h-BN-based materials in a PEC aptasensor. The charge transfer process was explained and verified using the ESR spin-trap technique (Fig. 4D). The PEC aptasensor recommended for DZN detection had a linear range of 0.01–10,000 nmol L^{-1}, a low LOD of 6.8 pmol L^{-1}.

Isocarbophos

ICB is a widely used OPs that has been used in China since the 1980s. This pesticide is used in agriculture to control insect populations, including locusts, by inhibiting acetylcholinesterase. Contamination of water with this pesticide causes poisoning of aquatic organisms such as *Gobiocypris rarus*, *Brachydanio rerio*, *Daphnia magna*, and *Oryzias latipes* [126–129]. Therefore, performing simple and sensitive methods for detecting, eliminating, and measuring ICB can increase food safety and preserve the environment. GC–MS and HPLC–MS [130, 131] have been used for sensitive soil measurements.

Yu et al. [132] designed an EC aptasensor on an Au electrode by modifying ICB-aptamer with 5′-SH-azobenzene and 3′-Fc groups for the sensitive determination of ICB. When this aptasensor was exposed to UV light, the *trans*-azobenzene structure *trans* formed to *cis*. With the addition of ICB, DPV current increased. The suggested aptasensor had a wide linear range of 10 pmol L^{-1} to 10 μmol L^{-1} under optimal conditions, with a LOD of 3 pmol L^{-1}. This aptasensor was also effectively used to validate applicability and stability in the ICB analysis of tomato samples, with a recovery rate of 76.2–119.3% and RSD of 1.8–10.7%.

Wang et al. [133] suggested an EC aptasensing approach based on UiO-66-NH_2 for ICB detection. The suggested MOF could bind to ICB-aptamers. The ICB-aptamers could undergo conformational changes and bind to them in the presence of ICB, preventing electron transfer to the electrode surface (Fig. 5A). This study demonstrates the significance of Zr sites and ligands in MOF structures for the development of extremely effective aptasensors. MOFs, as we know, have a large surface area and a variable pore environment, both of which can alter sensing effectiveness. The aptasensor responds to ICB linearly from 0.01 to 1 μg mL^{-1} with a LOD of 6 ng mL^{-1} (physical mixing) and from 0.001 to 1 μg mL^{-1} with a LOD of 0.9 ng mL^{-1} under optimal conditions (chemical combination). The results of ICB analysis in Chinese cabbage and apple peel samples were comparable, demonstrating its applicability. This work presents an alternative method for fabricating a food detection aptasensor based on UiO-66-NH_2.

By modifying an aptamer using MWCNTs and G-quadruplex, Li et al. [134] reported a FS aptasensor for ICB determination. At their respective terminals, the split ICB-aptamer was linked to a G-quadruplex in this study. In the presence of ICB, the split aptamers may conformationally change into a sandwiched-like ternary complex, preventing them from being adsorbed to MWCNTs because of increased steric hindrance. The FS analysis with a LOD of 10 nmol L^{-1} was used to determine ICB ranging from 10 to 500 nmol L^{-1}. The proposed aptasensor was utilized to detect ICB in Chinese cabbage and apple samples, with recoveries ranging from 97.8 to 106.4%, indicating that its great promise for assessing ICB.

Fan et al. [135] designed a FS aptasensor for the ICB detection based on AT-TWJ-DNA stabilized CuNP and magnetic Fe_3O_4@GO as FS signal and ssDNA adsorbent, respectively. The designed aptasensor had a high sensitivity to ICB under ideal conditions, with a low LOD of 3.38 nmol L^{-1} and a large linear dynamic range of 10–500 nmol L^{-1}. Furthermore, the aptasensor was successful in determining ICB in lake water and apple samples.

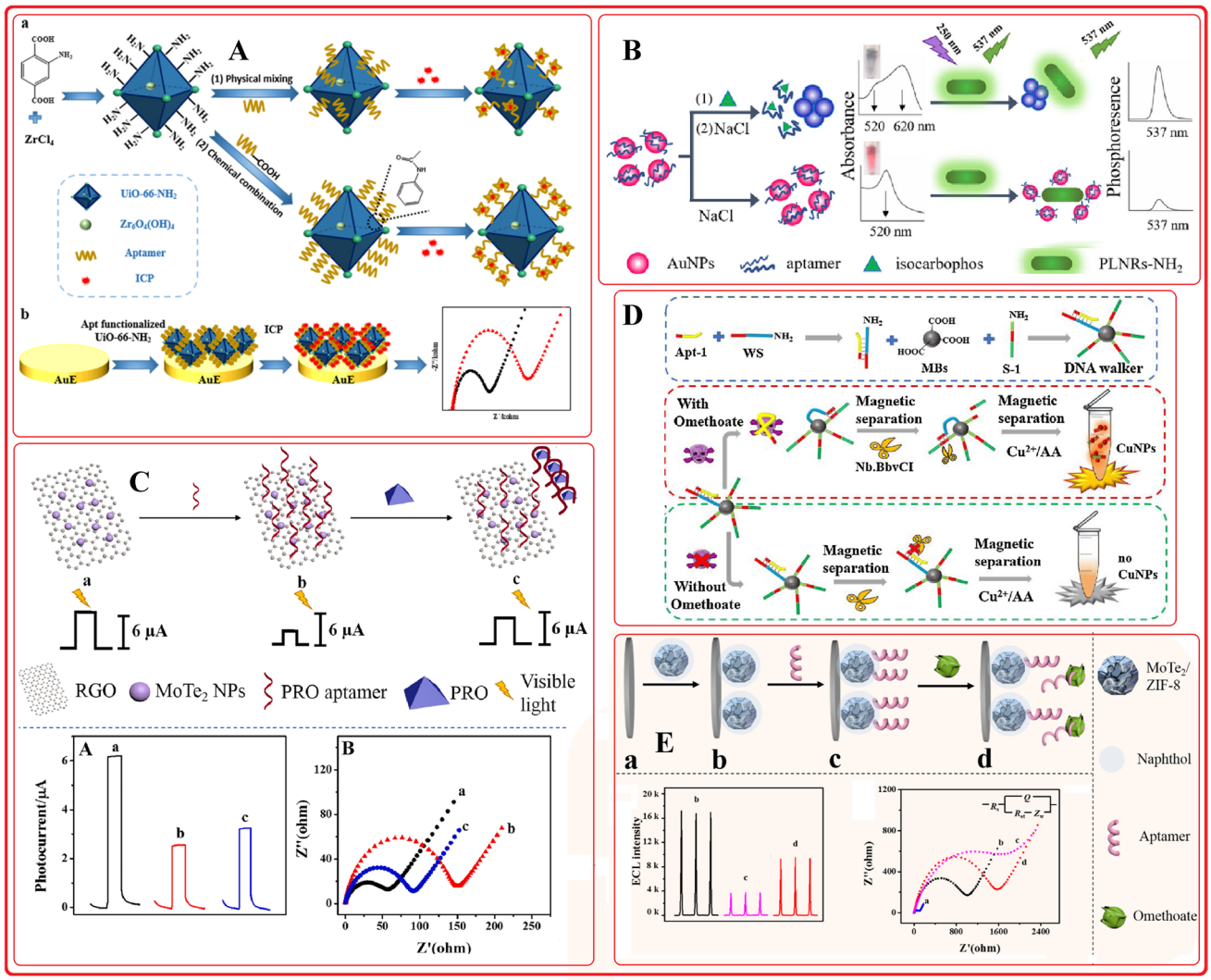

Fig. 5 **A** EC process of ICB detection based on UiO-66-NH_2 by Wang et al. [133], **B** schematic process of CM and PS aptasensor for ICB detection by Wang et al. [136], **C** PEC process of PFF detection based on $MoTe_2$NPs/RGO by Ding et al. [159], **D** FS process of OMT detection by Zhao et al. [169], and **E** schematic process of ECL aptasensor for OMT detection by Ding et al. [171]. Reprinted with permission from [133, 136, 159, 169], and [171]

Finally, Wang et al. [136] developed a new CM and PS aptasensor for sensitive ICB determination.

Phorate

The PhT (O,O-diethyl s-ethylthiomethylphosphorodithioate) is frequently used in agriculture due to its effectiveness against rodent pests such as mites, leafhoppers, leaf miners, nematodes, and rootworms. However, excessive use of this insecticide causes severe poisoning for animals and humans [137, 138]. Some methods such as GC [139], GC–MS [140, 141], and HPLC–MS [142, 143] have been applied for PhT detection.

Bala et al. [144] used a pesticide-specific aptamer as the recognition element and GNP as the optical sensor. The aptamer offers stability to the GNP when they are linked, ensuring their proper dissemination. However, when the PhT is added, the aptamer takes on a stiff conformation, causing the GNP to aggregate. The color of the solution changed from red to blue with the addition of PhT. The linear range and LOD of the developed CM aptasensor were 0.01 nmol L^{-1} – 1.3 μmol L^{-1} and 0.01 nmol L^{-1}, respectively. Finally, this aptasensing platform was compared with HPLC in spiked apple samples, with a recovery of 93–105%.

Li et al. [145] created an efficient aptasensor for the CM detection of PhT using DNA-AgNCs. PhT can cause DNA-AgNCs to aggregate; thus, the color of the solution changed from brown to colorless when it was added. A good linear relationship was found between altered absorbance and PhT concentration within 25 pg mL^{-1}–25 µg mL^{-1} under ideal conditions, and the LOD could reach 0.012 ng mL^{-1}. Furthermore, the suggested aptasensor was more accurate in quantifying PhT in spiked blood samples when compared with GC–MS.

Profenofos

PFF is used to control pests in vegetables, fruits and crops, especially lepidopteran species in cotton. According to the WHO, this pesticide is in the category of medium to toxic pesticides (class II) [146]. PFF is widely used in many parts of the world, especially in Asia, the Indian subcontinent, Africa and the Americas [147–149]. Himachal Pradesh, one of the northern states of India, as a major producer of apple, widely uses PFF to protect crops from pests and insects [150]. The improper use of this pesticide and its residue in environments such as surface water and soil has had negative consequences for both humans and the environment. Diagnostic methods such as GC [151, 152] and HPLC [153], which are devices with high prices and relatively large size, have been used. It has become critical in recent years to employ simple and low-cost approaches for PFF identification.

Using GNP/polyaniline g-SPE, Selvolini et al. [154] created a signal-off aptasensor for the EC detection of PFF. The hybridization reaction was assessed using a streptavidin–alkaline phosphatase enzyme combination that catalyzes the hydrolysis of 1-naphthyl-phosphate. The analytical response ranged from 0.1 to 10 µmol L^{-1} with a LOD of 0.27 µmol L^{-1}. Finally, with an 82–87% recovery, this aptasensing method was used to identify PFF in spiked pear juice samples.

Jiao et al. [155] designed another EC study. The probe's cleverly constructed HP structure was unraveled with PFF coupled with the aptamer sequences, and then, the target PFF and cDNA sequences containing HP were recycled separately using Vent polymerase and T7Exo. At the same time, the Fc-labeled DNA duplex could be digested into mononucleotides with the use of T7Exo, allowing the end-tagged Fc to contact the electrode surface and provide an increased EC response. As a result, within the PFF concentration range of 0.5–6.5 ng mL^{-1}, the proposed aptasensor had a LOD of 0.01 ng mL^{-1}. The devised method may be used to determine PFF residues in vegetables.

Zhang et al. [156] constructed a dual-amplification aptasensor for PFF detection by modifying a SPCE with an Au nanoshell and graphitized MWCNTs in the final examination of the EC aptasensor. Analytical performance assessment showed that the proposed aptasensor featured a calibration plot spanning the range of $0.1–1 \times 10^5$ ng mL^{-1} toward PFF and a LOD of 0.052 ng mL^{-1}. Furthermore, this aptasensor demonstrated good repeatability, selectivity, and stability, and performed well in vegetable samples.

Jin'en et al. [157] published a self-assembled aptamer with PEG-GO for the FS detection of PFF. The aptamer-PEG-GO showed better detection performance due to the grafting of the blocking agent PEG onto its surface, which improved biocompatibility and adjusted adsorption capacity. FS analysis with a LOD of 0.21 ng mL^{-1} was used to determine PFF levels ranging from 0.5 to 100 ng mL^{-1}. With recoveries of 90.8–114.2%, the proposed aptasensor was employed to detect PFF in milk, cabbage, and tap water samples.

Liu et al. [158] devised an ECL aptasensor for the detection of PFF. As a catalytic and luminescent system, AgNPs on PE and luminol-H_2O_2 were used, respectively. ECL detection signals were weakened when the aptamer made contact with the PFF, showing that the aptasensor had been successfully constructed. When PFF was introduced, it came into contact with the aptamer, resulting in a substantial reduction in ECL intensity. For the detection of PFF, the aptasensor had a large dynamic range of 0.5–100 ng mL^{-1} and a LOD of 0.13 ng mL^{-1} under ideal conditions. Finally, the aptasensor was used to detect PFF in grape and leaf lettuce samples.

Ding and colleagues [159] used $MoTe_2$NPs/RGO heterostructures with an appropriate Schottky barrier to produce sensitive PEC aptasensing technology for PFF detection (Fig. 5C). $MoTe_2$NPs/RGO heterostructures had photocurrent intensities of 21.8 and 10.5 higher than those of RGO and $MoTe_2$NPs, respectively. In this study, the co-immobilization of photovoltaic nanomaterials with PFF aptamer was able to create a suitable way to design a new sensitive aptasensor for PFF detection. The signal-to-noise ratio in this study has improved due to electrochemical measurements and has increased the sensitivity in measuring the PFF. The PEC aptasensor that resulted from the $MoTe_2$NPs/RGO heterostructures had a linear range of 1 ng L^{-1}–10 mg L^{-1} with a LOD of 0.33 ng L^{-1}. Two vegetables, including Chinese chive and potato, were used in the standard addition procedure. The RSD and recovery were 95.3–114% and 1.47–2.21%, respectively, indicating that the suggested PEC aptasensor may be used to analyze real samples.

Omethoate

Another type of OPs is OMT insecticide. This insecticide is also widely used to control agricultural pests. The mechanism of action of OMT, similar to other types of OPs, is by affecting on the secretion of the enzyme acetylcholinesterase,

which increases acetylcholine in the nervous system of the insect and controls its population [160, 161]. Despite the good performance of OMT insecticide to control agricultural pests, its excessive use in agricultural products has a negative impact on humans and environmental pollution, including surface water and soil [162, 163]. Therefore, various measurement methods have been used to detect OMT such as GC [164], HPLC–MS [165–167], and MS [168].

Zhao et al. [169] constructed a FS-OMT aptasensor using poly (T) stabilized CuNPs as the FS signal and a 3D-DNA walker as the signal amplifier. The aptasensor is composed of one strand of dsDNA and one strand of ssDNA immobilized on magnetic Fe_2O_3 beads. The dsDNA is hybridized by the target aptamer-contained DNA (Apt-1) and the partially cDNA, which acts as a WS in DNA walker. WS generates a free-walking ssDNA strand when OMT and Apt-1 bind specifically. With the help of nicking endonuclease, the 3D-DNA walker can produce a large amount of poly (T) DNA during WS. When the supernatant is combined with ascorbic acid and Cu^{2+}, poly (T)-templated CuNPs are formed, resulting in bright FS (Fig. 5D). Linear dynamic range from 5 to 200 nmol L^{-1} and a low LOD of 0.22 nmol L^{-1} were calculated. Furthermore, when utilized to detect OMT in cabbage, apple, and lake water samples, the selectivity and functionality imply that it could be beneficial in practical applications.

In another study of FS-OMT aptasensors, Nair et al. [170] built S-GQD using specialized recognition and binding capabilities of OMT-aptamer based on the tunable aggregation-disaggregation mechanism of S-GQD. The designed "signal-on" aptasensor could detect OMT in a linear range of 0.001 to 200 µg mL^{-1} with a LOD of 0.001 µg mL^{-1} under ideal conditions. This method showed excellent selectivity for detecting OMT.

Ding et al. [171] developed an ECL platform to detect OMT using $MoTe_2$ nanoparticles doped into ZIF-8. Electrocatalytic co-reactor $S_2O_8^{2}$ is easily converted to $SO_4^{\bullet -}$. As a result of faulty ZIF-8 catalysis, the ECL intensity of $MoTe_2$/ZIF-8 nanocomposites substantially increased compared with those of both ZIF-8 and $MoTe_2$ nanoparticles (Fig. 5E). Changes in ECL intensity as a function of relative OMT concentration were investigated further, and a linear range of 0.1 ng L^{-1} to 10 µg L^{-1} was achieved with a LOD of 0.033 ng L^{-1}. Furthermore, the ECL aptasensor appeared to have good practical performance in detecting potato and spinach extraction samples, suggesting a viable direction for building high-efficiency ECL aptasensors.

Wang et al. [172] created ssDNA-wrapped GNP that is resistant to aggregation caused by salt in this CM-OMT aptasensor. With an increase in OMT concentration from 0.1 to 10 µmol L^{-1}, the color shift during aggregation is plainly visible to the naked eye. The LOD of the CM aptasensor was 0.1 µmol L^{-1}. This method has been used to detect OMT in soil samples with great success. Table 2 summarizes different aptasensors for OP determination.

Conclusion and future perspectives

Pesticides containing OPs are used all over the world to avoid crop losses due to agricultural pests and to increase product production, quality, and appearance. Due to the expanding usage of OPs in agricultural production, they are becoming more problematic, highlighting the importance of developing an effective and sensitive OP detection system. OPs often stay in the soil and water environment for a long period at low concentrations and some of them may permeate into water bodies through various routes. The measurement of Ops becomes more difficult because of the very low concentrations and the complexity of soil and water matrix. As a result, developing a sensitive and reliable approach for monitoring OPs is critical for food safety and human health. The continuous concerns over the pesticides have become more alarming over the world to develop the novel detection techniques. As of now, OPs have been determined using a variety of analytical techniques (such as GC, CE, HPLC, spectrophotometry, and voltammetry) to meet increasing market and social requirement. Given their exceptional features, aptamers are good solutions for ultrasensitive detection in the creation of point-of-need devices. The ability to detect small compounds, ease of fabrication, stability, adaptability, reversibility of the binding, reusability, and significantly lower price, as well as the avoidance of animal hosts, are the key advantages. They have been utilized to build several types of aptasensors based on various detection techniques, such as EC and optical, because of the aforementioned features. However, aptasensors have promising future in determination of pesticide detection; there are sustainable challenges associated with each type of sensors. With their fast response, high sensitivity and specificity, low cost, and simple operation, EC aptasensors can enable multiplexed analysis and on-site detection. However, the stability of EC aptasensors should be increased, and samples must always be pretreated well. FS aptasensors may also provide high sensitivity detection with high efficiency, simplicity, and rapid analysis in a variety of samples. However, the FS life and background can affect the aptasensor's stability and accuracy. Also, CM aptasensors may provide clear viewing of results with naked eyes with convenience, practicality, and low cost, although they cannot perform quantitative and multiple detection without the use of other equipment and sensitivity must be further improved. Environmental variables like temperature and pH can affect the stability of the aptamer. The conjugation of the recognition element with the functionalized nanomaterial can increase the complexity, cost, and lifetime of the sensor. A comprehensive overview

Table 2 Aptasensors for organophosphate detection

OPs	Principle	Linear range	LOD	Interferences	Real samples	Ref
CHP	EC	1–10^5 ng mL^{-1}	0.33 ng mL^{-1}	Carbofuran, dichlorvos, phoxim	Leek, lettuce, pak choi	[49]
	EC	0.1–10^5 ng mL^{-1}	0.033 ng mL^{-1}	Phoxim, carbofuran, methyl parathion, carbaryl, acetamiprid	Leek, lettuce, pak choi, cabbage	[50]
	EC	0.1–150 ng mL^{-1}	70 pg mL^{-1}	Fenitrothion, OMT, deltamethrin, carbendazim, triazolone	Apple, celery, cabbage	[52]
	EC	1.0 fmol L^{-1}–0.4 pmol L^{-1}	0.35 fmol L^{-1}	Asulam, aflatoxin-B1, dimethoate, acetamiprid, carbofuran, MLT	Apple, lettuce	[57]
	EC	1.0 fmol L^{-1}–1.0 nmol L^{-1}	0.43 fmol L^{-1}	Glyphosate, acetamiprid, carbendazim, methamidophos	Tomato, apple	[59]
	EC	0.1–400 ng mL^{-1}	0.036 ng mL^{-1}	Amitrole, carbendazim, atrazine, fenitrothion	Apple, pak choi	[60]
	FS	100 pg mL^{-1}–100 μg mL^{-1}	0.73 ng mL^{-1}	Atrazine, carbaryl, acetamiprid, 2,4-D	Spinach, lettuce, cabbage	[61]
	FS	5–600 nmol L^{-1}	3.8 nmol L^{-1}	Carbofuran, dichlorvos, phoxim, acetamiprid	Tap water, cucumber, apple, cabbage, kiwifruit	[62]
	CM	0–1250 ng mL^{-1}	4.4 ng mL^{-1}	Atrazine, carbaryl, DZN, MLT, bisphenol A, 2,4-D	Winter jujube, cucumber, apple, cabbage	[63]
	ECL	10 nmol L^{-1}–1.0 fmol L^{-1}	0.35 fmol L^{-1}	Methyl parathion, carbendazim, cypermethrin, acetamiprid	Celery, apple, cabbage, tomato	[64]
MLT	EC	0.001 ng mL^{-1}–0.01 μg mL^{-1}	0.001 ng mL^{-1}	-	Lettuce leave, soil	[85]
	EC	0.5–600 ng L^{-1}	0.5 ng L^{-1}	Amitrole, CHP, methyl-parathion, deltamethrin, carbendazim, triazolone	Cauliflower, cabbage	[89]
	EC	0.1 fmol L^{-1}–1.0 μmol L^{-1}	0.5 fmol L^{-1}	CHP-methyl, DMT, Cu^{2+}, NO_3^-	Lettuce	[92]
	EC	25–850 ng L^{-1}	17.18 ng L^{-1}	CHP, fenitrothion, OMT, deltamethrin, carbendazim, triazolone	Long bean, cucumber	[95]
	FS	0.01 nmol L^{-1}–1 μmol L^{-1}	4 pmol L^{-1}	Atrazine, chlorsulfuron, CHP, diuron, 2,4-D	Tap water, lake water, soil water, orange	[96]
	FS	0.01–1 μmol L^{-1}	1.42 nmol L^{-1}	Parathion, thiamethoxam, methomyl, CHP, methamidophos, imidacloprid, acetamiprid	Tea powder, tap water	[97]
	CM	0.5–1000 pmol L^{-1}	0.06 pmol L^{-1}	Atrazine, chlorsulfuron, 2,4-D, diuron, PhT	Lake water, apple	[40]
	CM	0.01–0.75 nmol L^{-1}	1.94 pmol L^{-1}	Atrazine, CHP, chlorsulfuron, 2,4-D, diuron, ethion, PhT	Lake water, mineral water, apple	[9]
	CM	0.01–0.75 nmol L^{-1}	0.5 pmol L^{-1}	Atrazine, chlorsulfuron, 2,4-D, diuron, ethion, PhT	Tap water, lake water, apple	[98]
	CM	5 pmol L^{-1}–10 nmol L^{-1}	1 pmol L^{-1}	Atrazine, fenthion, parathion, PhT, chlorsulfuron, diuron, permethrin	Human serum	[99]
	ECL	1 pg L^{-1}–1 μg L^{-1}	0.3 pg L^{-1}	Carbendazim, cypermethrin, glyphosate, acetamiprid, aldicarb	Lake water, river water	[100]
	ECL	0.1 pmol L^{-1}–0.1 μmol L^{-1}	0.018 pmol L^{-1}	Acetamiprid, glyphosate, carbendazim, CHP, methionine	Tomato, apple	[101]
	UV–Vis	0–25 μg mL^{-1}	25 pg mL^{-1}	NaOH, $KHCO_3$, CH_3COOK, $NaHSO_4$, $C_2H_7NO_2$, $C_2H_2O_4$, barbital, diazepam, morphine, ketamine, dichlorvos, rogor, dipterex, CHP-methyl	Blood sample	[102]
	LC	0.8–50 pmol L^{-1}	2.5 pmol L^{-1}	Ethion, fenthion	Tap water, soil	[103]
	LC	1–600 nmol L^{-1}	0.465 nmol L^{-1}	Ethion, fenthion, fenobucarb, carbofuran, phosmet	Tap water, river water, apple	[104]

Table 2 (continued)

OPs	Principle	Linear range	LOD	Interferences	Real samples	Ref
DZN	EC	0.1–1000 nmol L^{-1}	0.0169 nmol L^{-1}	MLT, CHP, deltamethrin	Plasma	[120]
	EC	50 fmol L^{-1}–10 nmol L^{-1} 10 fmol L^{-1}–10 nmol L^{-1}	11 fmol L^{-1} 2 fmol L^{-1}	Indoxacarb, CHP, acetamiprid, imidacloprid, carbendazim, tebuconazole	River water, soil, apple, lettuce	[121]
	FS	1.05–206 nmol L^{-1}	0.13 nmol L^{-1}	Heptachlor, endrin, dieldrin, edifenphos, butachlor, chlordane	River water, cucumber, apple	[122]
	FS	0.05–500 ng mL^{-1}	0.023 ng mL^{-1}	Glyphosate, acetamiprid, chlorfenapyr, DZN	Tap water, tea, apple	[123]
	FS	4–31 nmol L^{-1}	0.4 nmol L^{-1}	Fenthion, dichlorvos, bentazon, pirimicarb, MLT, deltamethrin	Tap water, urine, river water, agricultural runoff water	[124]
	PEC	0.01–10,000 nmol L^{-1}	6.8 pmol L^{-1}	PhT, MLT, PFF, deltamethrin	Tap water, apple, river water	[125]
ICB	EC	10 pmol L^{-1}–10 μmol L^{-1}	3 pmol L^{-1}	Crotophos, DMT, imidacloprid, OMT, triazophos, profenophos, methamidophos, quinalphos	Tomato	[132]
	EC	0.01–1 μg mL^{-1} 0.001–1 μg mL^{-1}	6 ng mL^{-1} 0.9 ng mL^{-1}	Glucose, urea, citric acid, Mg^{2+}, NO_3^-	Chinese cabbage, apple peel	[133]
	FS	10–500 nmol L^{-1}	10 nmol L^{-1}	Methidathion, imidacloprid, CHP, phoxim, acetamiprid, thiram, diethofencarb, atrazine, metalaxyl, ziram	Chinese cabbage	[134]
	FS	10–500 nmol L^{-1}	3.38 nmol L^{-1}	Phoxim, CHP, imidacloprid, acetamiprid, methidathion	Lake water	[135]
	CM, PS	50–500 μg L^{-1} 5–160 μg L^{-1}	7.1 μg L^{-1} 0.54 μg L^{-1}	CHP, acetamiprid, imidacloprid, MLT, dichlorvos, K^+, Mg^{2+}, Fe^{3+}, Cu^{2+}, Al^{3+}	*Brassica rape*, Chinese cabbage, lettuce	[136]
PhT	CM	0.01 nmol L^{-1}–1.3 μmol L^{-1}	0.01 nmol L^{-1}	Atrazine, chlorsulfuron, 2,4-D, diuron, ethyl parathion	Apple	[144]
	CM	25 pg mL^{-1}–25 μg mL^{-1}	0.012 ng mL^{-1}	Barbital, diazepam, o-dimethyl-O-2, OMT, CHP-methyl, dipterex, morphine, ketamine, NaOH,$KHCO_3$, CH_3COOK, $NaHSO_3$, CH_3COONH_4, HOOCCOOH	Blood	[145]
PFF	EC	0.1–10 μmol L^{-1}	0.27 μmol L^{-1}	*p*-nitrophenyl-phosphate	Fruit juice	[154]
	EC	0.5–6.5 ng mL^{-1}	0.01 ng mL^{-1}	CHP, MLT, phoxim, parathion-methyl, ICB	Leek, lettuce, pak choi, cabbage	[155]
	EC	0.1–1 × 10^5 ng mL^{-1}	0.052 ng mL^{-1}	Monocrotophos, OMT; PhT, ICB, methamidophos	Spinach, lettuce, cabbage	[156]
	FS	0.5–100 ng mL^{-1}	0.21 ng mL^{-1}	CHP, MLT, phoxim, methyl parathion, OMT	Tap water, milk, cabbage	[157]
	ECL	0.5–100 ng mL^{-1}	0.13 ng mL^{-1}	OMT, monocrotophos, PhT	Leaf lettuce, rape	[158]
	PEC	1 ng L^{-1}–10 mg L^{-1}	0.33 ng L^{-1}	Edifenphos, DZN, OMT, pentachlorophenol	Chinese chive, potato	[159]
OMT	FS	5–200 nmol L^{-1}	0.22 nmol L^{-1}	ICB, PhT, PFF, methidathion, phoxim, paraoxon, CHP, MLT, acetamiprid, metalaxyl	Cabbage, apple, lake water	[169]
	FS	0.001–200 μg mL^{-1}	0.001 μg mL^{-1}	Carbofuran, methyl parathion, thiram		[170]
	ECL	0.1 ng L^{-1}–10 μg L^{-1}	0.033 ng L^{-1}	DZN, edifenphos, MLT, dichlorvos, PFF	Potato, spinach	[171]
	CM	0.1–10 μmol L^{-1}	0.1 μmol L^{-1}	PhT, PFF, ICB	Soil	[172]

of aptamer-based biosensors with different sensing strategies for OPs has been provided. The aptasensors discussed in this review are extremely selective and repeatable for detecting OPs in real samples, with the majority being built for sensitive and selective detection but further research and developments are still required.

After reviewing aptasensors for OP measurements in real samples, it was determined that new breakthroughs are still being made in the lab, with in situ deployment compatibility being promised but seldom delivered. Because the few sensors that have been fully integrated are still in the early stages of commercialization, significant data can only be gathered through the developer's measurements. EC sensors have the potential to revolutionize analysis programs, but bringing this scenario to fruition will take careful planning and dedicated study. Also, optical and EC sensors continue to limit the capacity to detect several pesticide residues in a single sensor. Hence, to overcome these challenges, further research can focus on:

(i) Controlled synthesis of nanomaterials with a small size distribution that will improve the performance of the sensor, while heterogeneous distribution decreases accuracy
(ii) Fabrication of portable miniaturized devices with wireless technology, long-term stability, and durability for on-site quantification
(iii) Sensing techniques and portable multiplexing devices that can be integrated into a fully automated system are in high demand
(iv) Miniaturized portable devices with minimal sample pretreatment or pre-separation that provide high-quality results will pave the way for a new generation of analytical devices capable of real-time detection.
(v) By incorporating sample pretreatment techniques such as solid phase extraction, it is possible to achieve successful separation and reduce the matrix effect in complex matrices.
(vi) For rapid on-site detection of pesticides, the use of paper-based sensors in conjunction with a portable device such as a smart phone can improve quantification capability and sensitivity, hence simplifying analysis, data recording, and dissemination.
(vii) Developing multi-channel optical devices capable of detecting multiple pesticide residues simultaneously in a single test
(viii) To be successfully commercialized, handheld optical devices must exhibit a high degree of accuracy and precision. The precision and accuracy of the optical device might be related to the well-established protocols used in conventional approaches.
(ix) Fabricating a ratiometric sensing platform with a dual recognition element for use in multiple sensing systems and for the purpose of reducing background noise and increasing stability.
(x) The use of aptasensors for pesticide detection is still in its infancy due to the restricted number of aptamers that have been developed so far. As a result, much work is required to improve pesticide aptamers through the use of split aptamers and other enrichment techniques.
(xi) Fabrication of environmentally safe, long-lasting, cost-effective, and robust sensing devices for real-time pesticide residue analysis. Additionally, while the sensing techniques have demonstrated a significant improvement in on-site detection of pesticide residue, their on-site usability and portability remain in development. Thus, future attempts should prioritize overcoming the aforementioned challenges. Aptamer, in conjunction with advancements in functional materials and nanomaterials, will open up a slew of new prospects for pesticide residue profiling.

Funding Hossein Khosropour is supported by the second century Fund (C2F) for Postdoctoral Fellowship, Chulalongkorn University.

Declarations

Conflict of interest The authors declare no competing interests.

References

1. Eddleston M, Buckley NA, Eyer P, Dawson AH (2008) Management of acute organophosphorus pesticide poisoning. Lancet 371:597–607. https://doi.org/10.1016/S0140-6736(07)61202-1
2. Songa EA, Okonkwo JO (2016) Recent approaches to improving selectivity and sensitivity of enzyme-based biosensors for organophosphorus pesticides: a review. Talanta 155:289–304. https://doi.org/10.1016/j.talanta.2016.04.046
3. Yan X, Li H, Su X (2018) Review of optical sensors for pesticides. Trac-Trend Anal Chem 103:1–20. https://doi.org/10.1016/j.trac.2018.03.004
4. Nougadère A, Reninger JC, Volatier JL, Leblanc JC (2011) Chronic dietary risk characterization for pesticide residues: a ranking and scoring method integrating agricultural uses and food contamination data. Food Chem Toxicol 49:1484–1510. https://doi.org/10.1016/j.fct.2011.03.024
5. Carvalho FP (2017) Pesticides, environment, and food safety. Food Energy Secur 6:48–60. https://doi.org/10.1002/fes3.108
6. Li TJ, Ding BQ, Zhou CX, Li DQ (2018) Treatment of organophosphorus pesticide wastewater using combinations of biodegradation bacteria. J Biobased Mater Bioenergy 12:525–531. https://doi.org/10.1166/jbmb.2018.1801
7. Liu KK, Dong HM, Deng Y (2016) Recent advances on rapid detection of pesticides based on enzyme biosensor of nanomaterials. J anosci Nanotechnol 16:6648–6656. https://doi.org/10.1166/jnn.2016.11392

8. Kaur R, Mavi GK, Raghav S, Khan I (2019) Pesticides classification and its impact on environment. Int J Curr Microbiol App Sci. 8(3):1889–1897. https://doi.org/10.20546/ijcmas.2019.803.224
9. Bala R, Dhingra S, Kumar M, Bansal K, Mittal S, Sharma RK, Wangoo N (2017) Detection of organophosphorus pesticide - malathion in environmental samples using peptide and aptamer based nanoprobes. Chem Eng J 311:111–116. https://doi.org/10.1016/j.cej.2016.11.070
10. Patel S, Sangeeta S (2019) Pesticides as the drivers of neuropsychotic diseases, cancers, and teratogenicity among agro-workers as well as general public. Environ Sci Pollut Res 26:91–100. https://doi.org/10.1007/s11356-018-3642-2
11. GarlitoB IM, Portolés T, Serrano R, Amlund H, Lundebye AK, Sanden M, Berntssen MHG, Hernández F (2019) LC-MS/MS method for the determination of organophosphorus pesticides and their metabolites in salmon and zebrafish fed with plant-based feed ingredients. Anal Bioanal Chem 411:7281–7291. https://doi.org/10.1007/s00216-019-02104-6
12. Yu C, Hao D, Chu Q, Wang T, Liu S, Lan T, Wang F, Pan C (2020) A one adsorbent QuEChERS method coupled with LC-MS/MS for simultaneous determination of 10 organophosphorus pesticide residues in tea. Food Chem 321:126657. https://doi.org/10.1016/j.foodchem.2020.126657
13. Masís-Mora M, Beita-Sandí W (2020) Validation of a methodology by LC-MS/MS for the determination of triazine, triazole and organophosphate pesticide residues in biopurification systems. J Chromatogr B 1156:122296. https://doi.org/10.1016/j.jchromb.2020.122296
14. Jullakan S, Bunkoed O, Pinsrithong S (2020) Solvent-assisted dispersive liquid-solid phase extraction of organophosphorus pesticides using a polypyrrole thin film-coated porous composite magnetic sorbent prior to their determination with GC-MS/MS. Microchim Acta 187:677. https://doi.org/10.1007/s00604-020-04649-1
15. Liu L, Yang M, He M, Liu T, Chen F, Li Y, Feng X, Zhang Y, Zhang F (2020) Magnetic solid phase extraction sorbents using methyl-parathion and quinalphos dual-template imprinted polymers coupled with GC-MS for class-selective extraction of twelve organophosphorus pesticides. Microchim Acta 187:503. https://doi.org/10.1007/s00604-020-04465-7
16. VaziriDozein S, Masrournia M, Es'haghi Z, Bozorgmehr MR, (2021) Development of a new magnetic dispersive solid-phase microextraction coupled with GC-MS for the determination of five organophosphorus pesticides from vegetable samples. Food Anal Methods 14:674–686. https://doi.org/10.1007/s12161-020-01906-0
17. Tang T, Deng J, Zhang M, Shi G, Zhou T (2016) Quantum dot-DNA aptamer conjugates coupled with capillary electrophoresis: a universal strategy for ratiometric detection of organophosphorus pesticides. Talanta 146:55–61. https://doi.org/10.1016/j.talanta.2015.08.023
18. Li J, Lu J, Qiao X, Xu Z (2017) A study on biomimetic immunoassay-capillary electrophoresis method based on molecularly imprinted polymer for determination of trace trichlorfon residue in vegetables. Food Chem 221:1285–1290. https://doi.org/10.1016/j.foodchem.2016.11.028
19. Li D, Jiang M, Xu L, Qiao X, Xu Z (2017) Simultaneous determination of acephate and isocarbophos in vegetables by capillary electrophoresis using ionic liquid and sodium dodecyl sulfate as modifiers. Food Anal Methods 10:3368–3374. https://doi.org/10.1007/s12161-017-0897-z
20. Gabaldón JA, Maquieira A, Puchades R (2007) Development of a simple extraction procedure for chlorpyrifos determination in food samples by immunoassay. Talanta 71:1001–1010. https://doi.org/10.1016/j.talanta.2006.04.041
21. Yin XL, Li YQ, Gu HW, Zhang Q, Zhang ZW, Li H, Li PW, Zhou Y (2021) Multicolor enzyme-linked immunosorbent sensor for sensitive detection of organophosphorus pesticides based on TMB^{2+}-mediated etching of gold nanorods. Microchem J 168:106411. https://doi.org/10.1016/j.microc.2021.106411
22 Tuerk C, Gold L (1990) Systematic evolution of ligands by exponential enrichment: RNA ligands to bacteriophage T4 DNA polymerase. Science. 249(4968):505–510. https://doi.org/10.1126/science.2200121
23. Blank M, Blind M (2005) Aptamers as tools for target validation. CurrOpin Chem Biol 9:336–342. https://doi.org/10.1016/j.cbpa.2005.06.011
24. Huang RR, Chen ZS, Liu M, Deng Y, Li S, He NY (2017) The aptamers generated from $HepG_2$ cells. Sci China Chem 60:786–792. https://doi.org/10.1007/s11426-016-0491-7
25. Meng HM, Liu H, Kuai HL, Peng RZ, Mo LT, Zhang XB (2016) Aptamer-integrated DNA nanostructures for biosensing, bioimaging and cancer therapy. Chem Soc Rev 45:2583–2602. https://doi.org/10.1039/C5CS00645G
26. Ellington AD, Szostak JW (1992) Selection in vitro of single-stranded DNA molecules that fold into specific ligand-binding structures. Nature 355:850–852. https://doi.org/10.1038/355850a0
27. Cox JC, Ellington AD (2001) Automated selection of anti-protein aptamers. Bioorg Med Chem 9:2525–2531. https://doi.org/10.1016/s0968-0896(01)00028-1
28. Berezovski M, Musheev M, Drabovich A (2006) Non-SELEX selection of aptamers. J Am Chem Soc 128:1410–1411. https://doi.org/10.1021/ja056943j
29. Tang J, Li J, Xiong P, Sun Y, Zeng Z, Tian X, Tang D (2020) Rolling circle amplification promoted magneto-controlled photoelectrochemical biosensor for organophosphorus pesticides based on dissolution of core-shell MnO_2nanoflower@CdS mediated by butyrylcholinesterase. Microchim Acta 187:450. https://doi.org/10.1007/s00604-020-04434-0
30. Song Y, Xu M, Li Z, HeL HuM, HeL ZhangZ, Du M (2020) Ultrasensitive detection of bisphenol A under diverse environments with an electrochemical aptasensor based on multicomponentAgMoheteronanostructure. Sens Actuators B Chem 321:128527. https://doi.org/10.1016/j.snb.2020.128527
31. Li S, Liu C, Han B, Luo J, Yin G (2017) An electrochemiluminescence aptasensor switch for aldicarb recognition via ruthenium complex-modified dendrimers on multiwalled carbon nanotubes. Microchim Acta 184:1669–1675. https://doi.org/10.1007/s00604-017-2177-4
32. Li J, Jiang D, Shan X, Wang W, Ou G, Jin H, Chen Z (2021) Determination of acetamiprid using electrochemiluminescentaptasensor modified by MoS_2QDs-PATP/PTCA and NH_2-UiO-66. Microchim Acta 188:44. https://doi.org/10.1007/s00604-021-04706-3
33. Xian-jin L, Cun-zheng Z, Yuan L, Li W, Qiu-hui H, Xian-jin L (2012) Selection of chlorpyrifos-binding ssDNA aptamer by SELEX. Jiangsu J Agric Sci 1:198–203
34. Barahona F, BardlivingCL PA, Bruno JG, Batt CA (2013) An aptasensor based on polymer-gold nanoparticle composite microspheres for the detection of malathion using surface-enhanced raman spectroscopy. Ind Biotechnol 9:42–50. https://doi.org/10.1089/ind.2012.0029
35. Jokar M, Safaralizadeh MH, Hadizadeh F, Rahmani F, Kalani MR (2017) Apta-nanosensor preparation and in vitro assay for rapid diazinon detection using a computational molecular approach. J Biomol Struct Dyn 35:343–353. https://doi.org/10.1080/07391102.2016.1140594
36. Wang L, Liu X, Zhang Q, Zhang C, Liu Y, Tu K, Tu J (2012) Selection of DNA aptamers that bind to four organophosphorus

pesticides. Biotechnol Lett 34:869–874. https://doi.org/10.1007/s10529-012-0850-6
37. Yuan R, Li HK, He H (2021) Recent advances in metal/covalent organic framework-based electrochemical aptasensors for biosensing applications. Dalton Trans 50:14091–14104. https://doi.org/10.1039/D1DT02360H
38. Su D, Li H, Yan X, Lin Y, Lu G (2021) Biosensors based on fluorescence carbon nanomaterials for detection of pesticides. TrAc-Trends Anal Chem 134:116126. https://doi.org/10.1016/j.trac.2020.116126
39. Bai W, Zhu C, Liu J, Yan M, Yang S, Chen A (2015) Gold nanoparticle-based colorimetric aptasensor for rapid detection of six organophosphorous pesticides. Environ Toxicol Chem 34:2244–2249. https://doi.org/10.1002/etc.3088
40. Bala R, Kumar M, Bansal K, Sharma RK, Wangoo N (2016) Ultrasensitive aptamer biosensor for malathion detection based on cationic polymer and gold nanoparticles. Biosens Bioelectron 85:445–449. https://doi.org/10.1016/j.bios.2016.05.042
41. Rigterink RH (1996) O pyridyl phosphates and phosphorothioates. U.S. Patent. 3:244 586
42. McCoy M (2011) Crop protection: India's Jubilant to commercialize new route to key insecticide intermediate. Chem Eng News 89:13. https://doi.org/10.1021/cen-v089n011.p013a
43. Ali D, Nagpure NS, Kumar S, Kumar R, Kushwaha B (2008) Genotoxicity assessment of acute exposure of chlorpyrifos to freshwater fish Channa punctatus (Bloch) using micronucleus assay and alkaline single-cell gel electrophoresis. Chemosphere 71:1823–1831. https://doi.org/10.1016/j.chemosphere.2008.02.007
44. TsagkarisaAS MD, Uttla L, Filippinic D, Pulkrabovaa J, Hajslova J (2021) A microfluidic paper-based analytical device (μPAD) with smartphone readout for chlorpyrifos-oxon screening in human serum. Talanta 222:121535. https://doi.org/10.1016/j.talanta.2020.121535
45. Akkaya E, Bozyiğit GD, Bakirdere S (2019) Simultaneous determination of 4-tert-octylphenol, chlorpyrifos-ethyl and penconazole by GC-MS after sensitive and selective preconcentration with stearic acid coated magnetic nanoparticles. Microchem J 146:1190–1194. https://doi.org/10.1016/j.microc.2019.01.077
46. Bodur S, Özlü C, Tışlı B, Fırat M, Selali D, Bakırdere CS (2020) Analytical protocol for determination of endosulfan beta, propham, chlorpyrifos, and acibenzolar-s-methyl in lake water and wastewater samples by gas chromatography-mass spectrometry after dispersive liquid–liquid microextraction. Environ Monit Assess 192:253. https://doi.org/10.1007/s10661-020-8214-5
47. Ramin M, Omidi F, Khadem M, Shahtaheri SJ (2021) Combination of dispersive solid-phase extraction with dispersive liquid-liquid microextraction followed by high-performance liquid chromatography for trace determination of chlorpyrifos in urine samples. Int J Environ Anal Chem 101:810–820. https://doi.org/10.1080/03067319.2019.1672670
48. Yang X, Wu X, Brown KA, Le T, Stice SL, Bartlett MG (2017) Determination of chlorpyrifos and its metabolites in cells and culture media by liquid chromatography-electrospray ionization tandem mass spectrometry. J Chromatograr B 1063:112–117. https://doi.org/10.1016/j.jchromb.2017.08.010
49. Jiao Y, Jia H, Guo Y, Zhang H, Wang Z, Sun X, Zhao J (2016) An ultrasensitive aptasensor for chlorpyrifos based on ordered mesoporous carbon/ferrocene hybrid multiwalled carbon nanotubes. RSC Adv 6:58541–58548. https://doi.org/10.1039/C6RA07735H
50. Jiao Y, Hou W, Fu J, Guo Y, Sun X, Wang X, Zhao J (2017) A nanostructured electrochemical aptasensor for highly sensitivedetection of chlorpyrifos. Sens Actuators B Chem 243:1164–1170. https://doi.org/10.1016/j.snb.2016.12.106
51. Asif M, Aziz A, Wang H, Wang Z, Wang W, Ajmal M, Xiao F, Chen X, Liu H (2019) Superlattice stacking by hybridizing layered double hydroxide nanosheets with layers of reduced graphene oxide for electrochemical simultaneous determination of dopamine, uric acid and ascorbic acid. Microchim Acta 186:61. https://doi.org/10.1007/s00604-018-3158-y
52. Xu G, Huo D, Hou C, Zhao Y, Bao J, Yang M, Fa H (2018) A regenerative and selective electrochemical aptasensor based on copper oxide nanoflowers-single walled carbon nanotubes nanocomposite for chlorpyrifos detection. Talanta 178:1046–1052. https://doi.org/10.1016/j.talanta.2017.08.086
53. Asif M, Aziz A, Ashraf G, Wang Z, Wang J, Azeem M, Chen X, Xiao F, Liu H (2018) Facet-inspired core-shell gold nanoislands on metal oxide octadecahedral heterostructures: high sensing performance toward sulfide in biotic fluids. ACS Appl Mater Interfaces 10:36675–36685. https://doi.org/10.1021/acsami.8b12186
54. Asif M, Ashraf G, Aziz A, Iftikhar T, Wang Z, Xiao F, Sun Y (2022) Tuning the redox chemistry of copper oxide nanoarchitectures integrated with rGOP via facet engineering: sensing H_2S toward SRB detection. ACS Appl Mater Interfaces 14:19480–19490. https://doi.org/10.1021/acsami.2c02119
55. Asif M, Wang H, Shuang D, Aziz A, Zhang G, Xiao F, Liu H (2017) Metal oxide intercalated layered double hydroxide nanosphere: with enhanced electrocatalyic activity towards H_2O_2 for biological applications. Sens Actuators B Chem 239:243–252. https://doi.org/10.1016/j.snb.2016.08.010
56. Gorodetsky AA, Buzzeo MC, Barton JK (2008) DNA-mediated electrochemistry. Bioconjugate Chem 19:2285–2296. https://doi.org/10.1021/bc8003149
57. Roushani M, Nezhadali A, Jalilian Z (2018) An electrochemical chlorpyrifos aptasensor based on the use of a glassy carbon electrode modified with an electropolymerized aptamer-imprinted polymer and gold nanorods. Microchim Acta 185:551. https://doi.org/10.1007/s00604-018-3083-0
58. Zhao X, Liu Y, Zuo J, Zhang J, Zhu L, Zhang J (2017) Rapid and sensitive determination of tartrazine using a molecularly imprinted copolymer modified carbon electrode (MIP-PmDB/PoPD-GCE). J Electroanal Chem 785:90–95. https://doi.org/10.1016/j.jelechem.2016.12.015
59. Liu J, Kong D, Liu Z, Liu H, Yi J, Tian D, Xia F, Zhou C (2020) Three-dimensional mesoporous dendritic fibrous nanosilica as a highly efficient DNA amplification platform for ultrasensitive detection of chlorpyrifos residues. Sens Actuators B Chem 319:128246. https://doi.org/10.1016/j.snb.2020.128246
60. Lin Z, Liu X, Li Y, Li C, Yang L, Ma K, Zhang Z, Huang H (2021) Electrochemical aptasensor based on Mo_2C/Mo_2N and gold nanoparticles for determination of chlorpyrifos. Microchim Acta 188:170. https://doi.org/10.1007/s00604-021-04830-0
61. Cheng N, Song Y, Fu Q, Du D, Luo Y, Wang Y, Xu W, Lin Y (2018) Aptasensor based on fluorophore-quencher nano-pair and smartphone spectrum reader for on-site quantification of multi-pesticides. Biosens Bioelectron 117:75–83. https://doi.org/10.1016/j.bios.2018.06.002
62. Liu Q, Wang H, Han P, Feng X (2019) Fluorescent aptasensing of chlorpyrifos based on assembly of cationic conjugated polymer-aggregated gold nanoparticles and luminescent metal-organic frameworks. Analyst 144:6025–6032. https://doi.org/10.1039/C9AN00943D
63. Liu Q, He Z, Wang H, Feng X, Han P (2020) Magnetically controlled colorimetric aptasensor for chlorpyrifos based on copper-based metal-organic framework nanoparticles with peroxidase mimetic property. Microchim Acta 187:524. https://doi.org/10.1007/s00604-020-04499-x

64. Liu J, Chen P, Xia F, Liu Z, Liu H, Yi J, Zhou C (2020) Sensitive electrochemiluminescence aptasensor for chlorpyrifos detection based on resonance energy transfer between MoS_2/CdS nanospheres and Ag/CQDs. Sens Actuators B Chem 315:128098. https://doi.org/10.1016/j.snb.2020.1280988
65. Alavinia SJ, Mirvaghefi AR, Farahmand H, Rafiee G, Alavinia SJ, Shiry N, Moodi S (2019) DNA damage, acetylcholinesterase activity, and hematological responses in rainbow trout exposed to the organophosphate malathion. Ecotoxicol Environ Saf 182:109311. https://doi.org/10.1016/j.ecoenv.2019.05.081
66. Chandra S (2008) Toxic effect of malathion on acetylcholinesterase activity of liver, brain and gills of freshwater catfish Heteropneustesfossilis. Environ Conserv J 9:47–52
67. Jebali J, Banni M, Guerbej H, Almeida EA, Bannaoui A, Boussetta H (2006) Effects of malathion and cadmium on acetylcholinesterase activity and metallothionein levels in the fish Seriola dumerilli. Fish Physiol Biochem 32:93–98. https://doi.org/10.1007/s10695-006-0041-2
68. Ortiz-Delgado JB, Funes V, Sarasquete C (2019) The organophosphate pesticide -OP- malathion inducing thyroidal disruptions and failures in the metamorphosis of the Senegalese sole. Solea senegalensis BMC Vet Res 15:57. https://doi.org/10.1186/s12917-019-1786-z
69. Lal B, Sarang MK, Kumar P (2013) Malathion exposure induces the endocrine disruption and growth retardation in the catfish, Clariasbatrachus (Linn.). Gen Comp Endocr 181:139–145. https://doi.org/10.1016/j.ygcen.2012.11.004
70. Ortiz-Delgado JB, Scala E, Arellano JM, Ubeda-Manzanaro M, Sarasquete C (2018) Toxicity of malathion at early life stages of the Senegalese sole, Solea senegalensis (Kaup, 1858): notochord and somatic disruptions. Histol Histopathol 33:157–169. https://doi.org/10.14670/HH-11-899
71. Inbaraj RM, Haider S (1988) Effect of malathion and endosulfan on brain acetylcholinesterase and ovarian steroidogenesis of Channa punctatus (Bloch). Ecotoxicol Environ Saf 16:123–128. https://doi.org/10.1016/0147-6513(88)90025-5
72. El-Nahhal Y (2018) Toxicity of some aquatic pollutants to fish. Environ Monit Assess 190:449. https://doi.org/10.1007/s10661-018-6830-0
73. Rico A, Waichman AV, Geber-Correa R, Van den Brink PJ (2011) Effects of malathion and carbendazim on Amazonian freshwater organisms: comparison of tropical and temperate species sensitivity distributions. Ecotoxicology 20:625–634. https://doi.org/10.1007/s10646-011-0601-9
74. Malhat F, Nasr I (2011) Organophosphorus pesticides residues in fish samples from the River Nile tributaries in Egypt. Bull Environ Contam Toxicol 87:689–692. https://doi.org/10.1007/s00128-011-0419-4
75. Fadaei A, Dehghani MH, Nasseri S, Mahvi AH, Rastkari N, Shayeghi M (2012) Organophosphorous pesticides in surface water of Iran. Bull Environ Contam Toxicol 88:867–869. https://doi.org/10.1007/s00128-012-0568-0
76. Gomez-Gutierrez AI, Jover E, Bodineau L, Albaies J, Bayona JM (2006) Organic contaminant loads into the Western Mediterranean Sea: estimate of Ebro River inputs. Chemosphere 65:224–236. https://doi.org/10.1016/j.chemosphere.2006.02.058
77. García-Ruiz C, Álvarez-Llamas G, Puerta Á, Blanco E, Sanz-Medel A, Marina ML (2005) Enantiomeric separation of organophosphorus pesticides by capillary electrophoresis. Anal Chim Acta 543:77–83. https://doi.org/10.1016/j.aca.2005.04.027
78. Liu Y, Liu S, Zhang Y, Qin D, Zheng Z, Zhu G, Lv Y, Liu Z, Dong Z, Liao X, Li X (2020) The degradation behaviour, residue distribution, and dietary risk assessment of malathion on vegetables and fruits in China by GC-FPD. Food Control 107:106754. https://doi.org/10.1016/j.foodcont.2019.106754
79. Lofty HM, Abd El-Aleem AA, Monir HH (2013) Determination of insecticides malathion and lambda-cyhalothrin residues in zucchini by gas chromatography. Bull Fac Pharm Cairo University 51:255–260. https://doi.org/10.1016/j.bfopcu.2013.08.001
80. Zhang A, Lai W, Sun J, Hu G, Liu W (2013) Probing the chiral separation mechanism and the absolute configuration of malathion, malaoxon and isomalathion enantiomers by chiral high performance liquid chromatography coupled with chiral detector-binding energy computations. J Chromatogr A 1281:26–31. https://doi.org/10.1016/j.chroma.2013.01.016
81. Bazmandegan-Shamili A, Haji Shabani AM, Dadfarnia S, Rohani Moghadam M, Saeidi M (2017) Preparation of magnetic mesoporous silica composite for the solid-phase microextraction of diazinon and malathion before their determination by high-performance liquid chromatography. J Sep Sci 40:1731–1738. https://doi.org/10.1002/jssc.201601339
82. Su R, Xu X, Wang X, Li D, Li X, Zhang H, Yu A (2011) Determination of organophosphorus pesticides in peanut oil by dispersive solid phase extraction gas chromatography-mass spectrometry. J Chromatogr B 879:3423–3428. https://doi.org/10.1016/j.jchromb.2011.09.016
83. Naushad Mu, ALOthman ZA, Khan MR, (2013) Removal of malathion from aqueous solution using De-Acidite FF-IP resin and determination by UPLC-MS/MS: equilibrium, kinetics and thermodynamics studies. Talanta 115:15–23. https://doi.org/10.1016/j.talanta.2013.04.015
84. Timofeeva I, Shishov A, Kanashina D, Dzema D, Bulatov A (2017) On-line in-syringe sugaring-out liquid-liquid extraction coupled with HPLC-MS/MS for the determination of pesticides in fruit and berry juices. Talanta 167:761–767. https://doi.org/10.1016/j.talanta.2017.01.008
85. Prabhakar N, Thakur H, Bharti A, Kaur N (2016) Chitosan-iron oxide nanocomposite based electrochemical aptasensor for determination of malathion. Anal Chim Acta 939:108–116. https://doi.org/10.1016/j.aca.2016.08.015
86. Asif M, Liu H, Aziz A, Wang H, Wang Z, Ajmal M, Xiao F, Liu H (2017) Core-shell iron oxide-layered double hydroxide: high electrochemical sensing performance of H_2O_2 biomarker in live cancer cells with plasma therapeutics. BiosensBioelectron 97:352–359. https://doi.org/10.1016/j.bios.2017.05.057
87. Asif M, Aziz A, Ashraf G, Iftikhar T, Sun Y, Xiao F, Liu H (2022) Unveiling microbiologically influenced corrosion engineering to transfigure damages into benefits: a textile sensor for H_2O_2 detection in clinical cancer tissues. Chem Eng J 427:131398. https://doi.org/10.1016/j.cej.2021.131398
88. Thakur H, Kaur N, Prabhakar N (2014) Metal oxide nanoparticle-embedded chitosan matrix based electrochemical detection of DNA hybridization. Bio Nano Sci 4:322–328. https://doi.org/10.1007/s12668-014-0154-5
89. Xu G, Hou J, Zhao Y, Bao J, Yang M, Fa H, Yang Y, Li L, Huo D, Hou C (2019) Dual-signal aptamer sensor based on polydopamine-gold nanoparticles and exonuclease I for ultrasensitive malathion detection. Sens Actuators B Chem 287:428–436. https://doi.org/10.1016/j.snb.2019.01.113
90. Selim Saleh MM, El-Sewify IM, Shenashen MA, Shahat A, Yamaguchi H, El-Safty SA, Khalil M (2017) Ratiometric fluorescent chemosensor for Zn^{2+} ions in environmental samples using supermicroporous organic-inorganic structures as potential platforms. Chem select. 2(34):11083–11090. https://doi.org/10.1002/slct.201702283
91. Hassen D, Shenashen MA, El-Safty AR, Elmarakbi A, El-Safty SA (2018) Anisotropic N-graphene-diffused Co_3O_4 nanocrystals with dense upper-zone top-on-plane exposure facets as effective ORR electrocatalysts. Sci Rep 8:3740. https://doi.org/10.1038/s41598-018-21878-w

92. Kaur N, Thakur H, Prabhakar N (2019) Multi walled carbon nanotubes embedded conducting polymer based electrochemical aptasensor for estimation of malathion. Microchem J 147:393–402. https://doi.org/10.1016/j.microc.2019.03.042
93. Asif M, Aziz A, Wang Z, Ashraf G, Wang J, Luo H, Chen X, Xiao F, Liu, (2019) Hierarchical CNTs@CuMn layered double hydroxide nanohybrid with enhanced electrochemical performance in H_2S detection from live cells. Anal Chem 91:3912–3920. https://doi.org/10.1021/acs.analchem.8b04685
94. Branzoi F, Branzoi V (2014) Nanocomposites based on conducting polymers and functionalized carbon nanotubes with different dopants obtained by electropolymerization. J Surf Eng Mater Adv Technol 4:164–179. https://doi.org/10.4236/jsemat.2014.43020
95. Xu G, Huo D, Hou J, Zhang C, Zhao Y, Hou C, Bao J, Yao X, Yang M (2021) An electrochemical aptasensor of malathion based on ferrocene/DNA-hybridized MOF, DNA coupling-gold nanoparticles and competitive DNA strand reaction. Microchem J 162:105829. https://doi.org/10.1016/j.microc.2020.105829
96 Bala R, Swami A, Tabujew I, Peneva K, Wangoo N, Sharma RK (2018) Ultra-sensitive detection of malathion using quantum dots-polymer based fluorescence aptasensor. BiosensBioelectron. 104:45–49. https://doi.org/10.1016/j.bios.2017.12.034
97. Chen Q, Sheng R, Wang P, Ouyang Q, Wang A, Ali S, Zareef M, Hassan MM (2020) Ultra-sensitive detection of malathion residues using FRET-based upconversion fluorescence sensor in food. Spectrochim Acta A Mol BiomolSpectrosc 241:118654. https://doi.org/10.1016/j.saa.2020.118654
98. Bala R, Mittal S, Sharma RK, Wangoo N (2018) A supersensitive silver nanoprobe based aptasensor for low cost detection of malathion residues in water and food samples. Spectrochim Acta A Mol Biomol Spectrosc 196:268–273. https://doi.org/10.1016/j.saa.2018.02.007
99. Abnous K, Danesh NM, Ramezani M, Alibolandi M, SarreshtehdarEmrani A, Lavaee P, Taghdisi SM (2018) A colorimetric gold nanoparticle aggregation assay for malathion based on target-induced hairpin structure assembly of complementary strands of aptamer. Microchim Acta 85:216. https://doi.org/10.1007/s00604-018-2752-3
100. Chen P, Liu Z, Liu J, Liu H, Bian W, Tian D, Xia F, Zhou C (2020) A novel electrochemiluminescence aptasensor based CdTeQDs@NH_2-MIL-88(Fe) for signal amplification. Electrochim Acta 354:136644. https://doi.org/10.1016/j.electacta.2020.136644
101. Liu H, Liu Z, Yi J, Ma D, Xia F, Tian D, Zhou C (2021) A dual-signal electroluminescence aptasensor based on hollow Cu/ Co-MOF-luminol and g-C_3N_4 for simultaneous detection of acetamiprid and malathion. Sens Actuators B Chem 331:129412. https://doi.org/10.1016/j.snb.2020.129412
102. Chen C, Shi J, Guo Y, Zha L, Lan L, Chang Y, Ding Y (2018) A novel aptasensor for malathion blood samples detection based on DNA-silver nanocluster. Anal Methods 10:1928–1934. https://doi.org/10.1039/c8ay00428e
103. Kim Hong PT, Jang C-H (2020) Sensitive and label-free liquid crystal-based optical sensor for the detection of malathion. Anal Biochem 593:113589. https://doi.org/10.1016/j.ab.2020.113589
104. Nguyen DK, Jang C-H (2021) A cationic surfactant-decorated liquid crystal-based aptasensor for label-free detection of malathion pesticides in environmental samples. Biosensors 11:92. https://doi.org/10.3390/bios11030092
105. CycońM WM, Piotrowska-Seget Z (2009) Biodegradation of the organophosphorus insecticide diazinon by Serratia sp. and Pseudomonas sp. and their use in bioremediation of contaminated soil. Chemosphere 76:494–501. https://doi.org/10.1016/j.chemosphere.2009.03.023
106. Harper B, Luukinen B, Gervais JA, Buhl K, Stone D (2009) Diazinon general fact sheet, national pesticide information center, Oregon State University Extension Services. http://npic.orst.edu/factsheets/Diazgen.html.
107. Shah MD, Iqbal M (2010) Diazinon-induced oxidative stress and renal dysfunction in rats. Food Chem Toxicol 48:3345–3353. https://doi.org/10.1016/j.fct.2010.09.003
108. Ezemonye L, Ikpesu T, Tongo I (2008) Distribution of diazinon in water, sediment and fish from Warri River, Niger Delta, Nigeria, Jordan. J Biol Sci 1:77–83
109. Poet TS, Kousba AA, Dennison SL, Timchalk C (2004) Physiologically based pharmacokinetic/pharmacodynamic model for the organophosphorus pesticide diazinon. Neurotoxicology 25:1013–1030. https://doi.org/10.1016/j.neuro.2004.03.002
110. Khodadadi M, Samadi M, Rahmani A, Maleki R, Allahresani A, Shahidi R (2010) Determination of organophosphorous and carbamat pesticides residue in drinking water resources of Hamadan in 2007. Iran. J Health Environ 2:250–257. http://ijhe.tums.ac.ir/article-1-143-en.html
111. Pirsaheb M, Dargahi A (2016) Performance of granular activated carbon to diazinon removal from aqueous solutions. J Environ Sci Technol 18:117–126
112. Bavcon M, Trebše P, Zupančič-Kralj L (2003) Investigations of the determination and transformations of diazinon and malathion under environmental conditions using gas chromatography coupled with a flame ionisation detector. Chemosphere 50:595–601. https://doi.org/10.1016/S0045-6535(02)00643-4
113. Akhlaghi H, Motavalizadehkakhky A, Emamiyan R (2013) Determination of diazinon in fruits from northeast of Iran using the QuEChERS sample preparation method and GCMS. Asian J Chem. 25:1727–1729. https://doi.org/10.14233/ajchem.2013.14244
114. Blasco C, Vazquez-Roig P, Onghena M, Masia A, Picó Y (2011) Analysis of insecticides in honey by liquid chromatography–ion trap-mass spectrometry: comparison of different extraction procedures. J Chromatogr A 1218:4892–4901. https://doi.org/10.1016/j.chroma.2011.02.045
115. Salm P, Taylor PJ, Roberts D, de Silva J (2009) Liquid chromatography-tandem mass spectrometry method for the simultaneous quantitative determination of the organophosphorus pesticides dimethoate, fenthion, diazinon and chlorpyrifos in human blood. J Chromatogr B 877:568–574. https://doi.org/10.1016/j.jchromb.2008.12.066
116. Sánchez ME, Méndez R, Gómez X, Martín-Villacorta J (2003) Determination of diazinon and fenitrothion in environmental water and soil samples by HPLC. J LiqChromatogrRelat Technol 26:483–497. https://doi.org/10.1081/JLC-120017184
117. Soodi M, Garshasbi A, Eskandari S (2013) Development a HPLC method for simultaneous determination of azinphose methyl, diazinon, phosalone and chlorpyrifos residues in fruit. J Pharm Heal Sci 1:279–287. https://www.sid.ir/en/journal/ViewPaper.aspx?ID=377632
118. Kharbouchec L, Gil Garcíaab MD, Lozanoab A, Hamaizic H, Martínez Galera M (2019) Solid phase extraction of pesticides from environmental waters using an MSU-1 mesoporous material and determination by UPLC-MS/MS. Talanta 199:612–619. https://doi.org/10.1016/j.talanta.2019.02.092
119. Chang PL, Hsieh MM, Chiu TC (2016) Recent advances in the determination of pesticides in environmental samples by capillary electrophoresis. Int J Environ Res Public Health 13:409. https://doi.org/10.3390/ijerph13040409
120. Hassani S, Rezaei Akmal M, Salek-Maghsoudi A, Rahmani S, Ganjali MR, Norouzi P, Abdollahi M (2018) Novel label-free electrochemical aptasensor for determination of diazinon using

gold nanoparticles-modified screen-printed gold electrode. Biosens Bioelectron 120:122–128. https://doi.org/10.1016/j.bios.2018.08.041
121. Khosropour H, Rezaei B, Rezaei P, Ensafi AA (2020) Ultrasensitive voltammetric and impedimetric aptasensor for diazinon pesticide detection by VS_2 quantum dots-graphene nanoplatelets/carboxylated multiwalled carbon nanotubes as a new group nanocomposite for signal enrichment. Anal Chim Acta 1111:92–102. https://doi.org/10.1016/j.aca.2020.03.047
122. Arvand M, Mirroshandel AA (2019) An efficient fluorescence resonance energy transfer system from quantum dots to graphene oxide nano sheets: application in a photoluminescence aptasensing probe for the sensitive detection of diazinon. Food Chem 280:115–122. https://doi.org/10.1016/j.foodchem.2018.12.069
123. Rong Y, Li H, Ouyang Q, Ali S, Chen Q (2020) Rapid and sensitive detection of diazinon in food based on the FRET between rare-earth doped upconversion nanoparticles and graphene oxide. Spectrochim Acta A Mol Biomol Spectrosc 239:118500. https://doi.org/10.1016/j.saa.2020.118500
124. Fooladi Talari F, Bozorg A, Faridbod F, Vossoughi M (2021) A novel sensitive aptamer-based nanosensor using rGQDs and MWCNTs for rapid detection of diazinon pesticide. J Environ Chem Eng 9:104878. https://doi.org/10.1016/j.jece.2020.104878
125. Tan J, Peng B, Tang L, Feng C, Wang J, Yu J, Ouyang X, Zhu X (2019) Enhanced photoelectric conversion efficiency: a novel h-BN based self powered photoelectrochemical aptasensor for ultrasensitive detection of diazinon. Biosens Bioelectron 142:111546. https://doi.org/10.1016/j.bios.2019.111546
126. Lin KD, Liu WP, Li L, Gan J (2008) Single and joint acute toxicity of isocarbophosenantiomers to daphnia magna. J Agric Food Chem 56:4273–4277. https://doi.org/10.1021/jf073535l
127. Liu H, Liu J, Xu L, Zhou S, Li L, Liu W (2010) Enantioselective cytotoxicity of isocarbophos is mediated by oxidative stress-induced JNK activation in human hepatocytes. Toxicology 276:115–121. https://doi.org/10.1016/j.tox.2010.07.018
128. Di S, Cang T, Qi P, Wang X, Xu M, Wang Z, Xu H, Wang Q, Wang X (2019) A systemic study of enantioselectivity of isocarbophos in rice cultivation: enantioselective bioactivity, toxicity, and environmental fate. J Hazard Mater 375:305–311. https://doi.org/10.1016/j.jhazmat.2019.05.002
129. Di S, Cang T, Qi PP, Wang ZW, Wang XY, Xu MF, Wang XQ, Xu H, Wang Q (2019) Comprehensive study of isocarbophos to various terrestrial organisms: enantioselective bioactivity, acute toxicity, and environmental behaviors. J Agric Food Chem 67:10997–11004. https://doi.org/10.1021/acs.jafc.9b02931
130. Cacho JI, CampilloN VP, Hernández-Córdoba M (2018) In situ ionic liquid dispersive liquid-liquid microextraction coupled to gas chromatography-mass spectrometry for the determination of organophosphorus pesticides. J Chromatogr A 1559:95–101. https://doi.org/10.1016/j.chroma.2017.12.059
131. Qi P, Wang X, Zhang H, Wang X, Xu H, Wang Q (2015) Rapid enantioseparation and determination of isocarbophos enantiomers in orange pulp, peel, and kumquat by chiral HPLC-MS/MS. J Food Anal Method 8:531–538. https://doi.org/10.1007/s12161-014-9922-7
132. Yu M, Chang Q, Zhang L, Huang Z, Song C, Chen Y, Wu X, Lu Y (2021) Ultra-sensitive detecting OPs-isocarbophos using photoinduced regeneration of aptamer-based electrochemical sensors. Electroanalysis 33:1–7. https://doi.org/10.1002/elan.202100222
133. Wang N, Liu Z, Wen L, Zhang B, Tao C, Wang J (2022) Aptamer-binding zirconium-based metal-organic framework composites prepared by two conjunction approaches with enhanced bio-sensing for detecting isocarbophos. Talanta 236:122822. https://doi.org/10.1016/j.talanta.2021.122822
134. Li X, Tang X, Chen X, Qu B, Lu L (2018) Label-free and enzyme-free fluorescent isocarbophosaptasensor based on MWCNTs and G-quadruplex. Talanta 188:232–237. https://doi.org/10.1016/j.talanta.2018.05.092
135. Fan K, Yang R, Zhao Y, Zang C, Miao X, Qu B, Lu L (2020) A fluorescent aptasensor for sensitive detection of isocarbophos based on AT-rich three-way junctions DNA templated copper nanoparticles and Fe_3O_4@GO. Sens Actuators B Chem 321:128515. https://doi.org/10.1016/j.snb.2020.128515
136. Wang RH, Zhu CL, Wang LL, Xu LZ, Wang WL, Yang C, Zhang Y (2019) Dual-modal aptasensor for the detection of isocarbophos in vegetables. Talanta 205:120094. https://doi.org/10.1016/j.talanta.2019.06.094
137. Devine GJ, Furlong MJ (2007) Insecticide use: contexts and ecological consequences. Agric Hum Values 24:281–306. https://doi.org/10.1007/s10460-007-9067-z
138. Kumar N, Pathera AK, Saini P, Kumar M (2012) Harmful effects of pesticides on human health. Ann Agri Bio Res 17:125–127
139. Yu C, Hu B (2009) Sol-gel polydimethylsiloxane/poly(vinylalcohol)-coated stir bar sorptive extraction of organophosphorus pesticides in honey and their determination by large volume injection GC. J Sep Sci 32:147–153. https://doi.org/10.1002/jssc.200800486
140. Ramasubramanian T, Paramasivam M (2016) Dissipation behavior of phorate and its toxic metabolites in the sandy clay loam soil of a tropical sugarcane ecosystem using a single-step sample preparation method and GC-MS. J Sep Sci 39:3973–3982. https://doi.org/10.1002/jssc.201600560
141. Alkan E, Kapukıran F, Öztürk Er E, Chormey DS, Keyf S, Özdoğan N, Bakırdere S (2018) Simultaneous determination of phorate and oxyfluorfen in well water samples with high accuracy by GC-MS after binary dispersive liquid-liquid microextraction. Water Air Soil Pollut 229:298. https://doi.org/10.1007/s11270-018-3939-2
142. Xu ZL, Deng H, Deng XF, Yang JY, Jiang YM, Zeng DP, Huang F, Shen YD, Lei HT, Wang H, Sun YM (2012) Monitoring of organophosphorus pesticides in vegetables using monoclonal antibody-based direct competitive ELISA followed by HPLC-MS/MS. Food Chem 131:1569–1576. https://doi.org/10.1016/j.foodchem.2011.10.020
143. Ko AY, Kim H, Jang J, Lee EH, Ju Y, Noh M, Kim S, Park SW, Chang MI, Rhee GS (2015) Development of an official analytical method for determination of phorate and its metabolites in livestock using LC-MS/MS. J Food Hyg Saf. 30:272–280. https://doi.org/10.13103/JFHS.2015.30.3.272
144. Bala R, Sharma RK, Wangoo N (2016) Development of gold nanoparticles-based aptasensor for the colorimetric detection of organophosphorus pesticide phorate. Anal Bioanal Chem 408:333–338. https://doi.org/10.1007/s00216-015-9085-4
145. Li X, Shi J, Chen C, Li W, Han L, Lan L, Guo Y, Chang Y, Cai J, Ding Y (2018) One-step, visual and sensitive detection of phorate in blood based on a DNA-AgNCaptasensor. New J Chem 42:6293–6298. https://doi.org/10.1039/C8NJ00958A
146. WHO (2010) The WHO recommended classification of pesticides by hazard and guidelines to classification 2009.
147. Li X, Li S, Liu S, Zhu G (2010) Lethal effect and in vivo genotoxicity of profenofos to Chinese native amphibian (Rana spinosa) tadpoles. Arch Environ Contam Toxicol 59:478–483. https://doi.org/10.1007/s00244-010-9495-4
148. Swarnam TP, Velmurugan A (2013) Pesticide residues in vegetable samples from the Andaman Islands. India Environ Monit Assess 185:6119–6127. https://doi.org/10.1007/s10661-012-3012-3
149. Loutfy N, Fuerhacker M, Lesueur C, Gartner M, Ahmed MT, Mentler A (2008) Pesticide and non-dioxin-like polychlorinated

biphenyls (NDL-PCBs) residues in foodstuffs from Ismailia city. Egypt Food Addit Contam 1:32–40. https://doi.org/10.1080/19393210802236885
150. Sharma ID, Nath A (2003) Persistence of different pesticides in apple. VII International Symposium on Temperate Zone Fruits in the Tropics and Subtropics-Part Two. 696:437–440. https://doi.org/10.17660/ActaHortic.2005.696.78
151. Hoisang W, Nacapricha D, Wilairat P, Tiyapongpattana W (2019) Solidification of floating organic droplet microextraction for determination of seven insecticides in fruit juice, vegetables and agricultural runoff using gas chromatography with flame ionization and mass spectrometry detection. J Sep Sci 42:2032–2043. https://doi.org/10.1002/jssc.201801193
152. Pawar UD, Pawar CD, Kulkarni UK, Pardeshi RK (2020) Development method of high-performance thin-layer chromatographic detection of synthetic organophosphate insecticide profenofos in visceral samples. JPC-J Planar Chromat 33:203–206. https://doi.org/10.1007/s00764-020-00015-2
153. Mahajan R, Chatterjee S (2018) A simple HPLC-DAD method for simultaneous detection of two organophosphates, profenofos and fenthion, and validation by soil microcosm experiment. Environ Monit Assess 190:327. https://doi.org/10.1007/s10661-018-6710-7
154. Selvolini G, Bajan I, Hosu O, Cristea C, Sandulescu R, Marrazza G (2018) DNA-Based sensor for the detection of an organophosphorus pesticide: profenofos. Sensors 18:2035. https://doi.org/10.3390/s18072035
155. Jiao Y, Fu J, Hou W, Shi Z, Guo Y, Sun X, Yang Q, Li F (2018) Homogeneous electrochemical aptasensor based on a dual amplification strategy for sensitive detection of profenofos residues. New J Chem 42:14642–14647. https://doi.org/10.1039/C8NJ02262C
156. Zhang H, Sun J, Cheng S, Liu H, Li F, Guo Y, Sun X (2020) A dual-amplification electrochemical aptasensor for profenofos detection. J Electrochem Soc 167:027515. https://doi.org/10.1149/1945-7111/ab6972]
157. Jin'en X, Shuang L, Yi L, Yingli C, Yu L, Junlan G,Jiahui J, Yaoling X, Xiaohui X (2020) Fluorescent aptamer-polyethylene glycol functionalized graphene oxide biosensor for profenofos detection in food. Chem. Res. Chinese Universities 36:787-794. https://doi.org/10.1007/s40242-019-9257-4
158. Liu H, Cheng S, Shi X, Zhang H, Zhao Q, Dong H, Guo Y, Sun X (2019) Electrochemiluminescence aptasensor for profenofos detection based on silver nanoparticles enhanced luminol luminescence system. J Electrochem Soc 166:B1562–B1566. https://doi.org/10.1149/2.0801915jes
159. Ding L, Wei J, Qiu Y, Wang Y, Wen Z, Qian J, Hao N, Ding C, Li Y, Wang K (2021) One-step hydrothermal synthesis of telluride molybdenum/reduced graphene oxide with Schottky barrier for fabricating label-free photoelectrochemical profenofosaptasensor. Chem Eng J 407:127213. https://doi.org/10.1016/j.cej.2020.127213
160. Zhang C, Lin B, Cao Y, Guo M, Yu Y (2017) Fluorescence determinationof omethoate based on a dual strategy for improving sensitivity. J Agric Food Chem 65:3065–3073. https://doi.org/10.1021/acs.jafc.7b00166
161. Zhang Q, Yu Y, Yun X, Luo B, Jiang H, Chen C, Wang S, Min D (2020) Multicolor colorimetric sensor for detection of omethoate based on the inhibition of the enzyme-induced metallization of gold nanorods. ACS Appl Nano Mater 3:5212–5219. https://doi.org/10.1021/acsanm.0c00641
162. Song D, Li Q, Lu X, Li Y, Li Y, Wang Y, Gao F (2018) Ultra-thin bimetallic alloy nanowires with porous architecture/monolayer MoS_2 nanosheet as a highly sensitive platform for the electrochemical assay of hazardous omethoate pollutant. J Hazard Mater 357:466–474. https://doi.org/10.1016/j.jhazmat.2018.06.021
163. Ma L, Zhou L, He Y, Wang L, Huang Z, Jiang Y, Gao J (2018) Mesoporous bimetallic PtPd nanoflowers as a platform to enhance electrocatalytic activity of acetylcholinesterase for organophosphate pesticide detection. Electroanalysis 30:1801–1810. https://doi.org/10.1002/elan.201700845
164. Lin DZ, Ming SM, Guang YC, Hua PY, Juan CJ (2015) Research of omethoate residue in broccoli and validation studies by GC-FPD and GC-MS-EI methods. J Food Saf Quality 6:86–92
165. John H, Eddleston M, Clutton RE, Worek F, Thiermann H (2010) Simultaneous quantification of the organophosphorus pesticides dimethoate and omethoate in porcine plasma and urine by LC-ESI-MS/MS and flow-injection-ESI-MS/MS. J Chromatogr B 878:1234–1245. https://doi.org/10.1016/j.jchromb.2010.01.003
166. Jayatilaka NK, Montesano MA, Whitehead RD Jr, Schloth SJ, Needham LL, Barr DB (2011) High-throughput sample preparation for the quantitation of acephate, methamidophos, omethoate, dimethoate, ethylenethiourea, and propylenethiourea in human urine using 96-well-plate automated extraction and high-performance liquid chromatography-tandem mass spectrometry. Arch Environ Contam Toxicol 61:59–67. https://doi.org/10.1007/s00244-010-9593-3
167. Hrynko I, Łozowicka B, Kaczyński P (2019) Comprehensive analysis of insecticides in melliferous weeds and agricultural crops using a modified QuEChERS/LC-MS/MS protocol and of their potential risk to honey bees (Apis mellifera L.). Sci Total Environ 657:16–27. https://doi.org/10.1016/j.scitotenv.2018.11.470
168. Liu A, Kou W, Zhang H, Xu J, Zhu L, Kuang S, Huang K, Chen H, Jia Q (2020) Quantification of trace organophosphorus pesticides in environmental water via enrichment by magnetic-zirconia nanocomposites and online extractive electrospray ionization mass spectrometry. Anal Chem 92:4137–4145. https://doi.org/10.1021/acs.analchem.0c00304
169. Zhao Y, Wang Y, Yang R, Zhang H, Zhao Y, Miao X, Lu L (2021) A zero-background fluorescent aptasensor for ultrasensitive detection of pesticides based on magnetic three-dimensional DNA walker and poly(T)-templated copper nanoparticles. Sens Actuators B Chem 343:130172. https://doi.org/10.1016/j.snb.2021.130172
170. Nair RV, Chandran PR, Mohamed AP, Pillai S (2021) Sulphur-doped graphene quantum dot based fluorescent turn-on aptasensor for selective and ultrasensitive detection of omethoate. Anal Chim Acta 1181:338893. https://doi.org/10.1016/j.aca.2021.338893
171. Ding L, Hong H, Xiao L, Hu Q, Zuo Y, Hao N, Wei J, Wang K (2021) Nanoparticles-doped induced defective ZIF-8 as the novel cathodic luminophore for fabricating high-performance electrochemiluminescence aptasensor for detection of omethoate. Biosens Bioelectron 192:113492. https://doi.org/10.1016/j.bios.2021.113492
172. Wang P, Wan Y, Ali A, Deng S, Su Y, Fan C, Yang S (2016) Aptamer-wrapped gold nanoparticles for the colorimetric detection of omethoate. Sci China Chem 59:237–242. https://doi.org/10.1007/s11426-015-5488-5